Table of Contents

Table of Contents

List of Figures

List of Figures

List of Tables

1. INTRODUCTION

NASA and RSC-E are involved in a cooperative venture in which the Shuttle will rendezvous with the Mir Space Station during several missions over the next two years. This sequence of at least six missions will serve as a precursor to the two nations' involvement in the International Space Station. The rendezvous missions provide NASA scientists and engineers an opportunity to study the orbital, dynamic, and environmental conditions of long duration spacecraft, as well as develop evaluation and risk mitigation techniques which have direct application to the International Space Station.

STS-74 launched on November 12, 1995, and was docked to the Mir Station from the 14th thru the 17th. The nine day mission ended with a KSC landing on November 20, 1995. This was the Shuttle's second docking mission and its third rendezvous with the Mir Station. Approximately 1030 photographs and 22 hours of video of the Mir Station were acquired during the mission. This report documents results from several survey-related analysis tasks.

Results of Detailed Test Objective (DTO-1118) analysis from STS-63 and STS-71 were documented in earlier reports. The STS-63 JSC/RSC-E Mir Survey Joint Report (JSC # 27246) was released in September 1995 and the STS-71 JSC/RSC-E Mir Survey Joint Report (JSC # 27355) is currently in distribution. Both of these reports include evaluation of the Mir imagery by RSC-Energia.

1.1 Overview of Mir Photo/TV Survey

DTO-1118 integrates the requirements for photographic and video imagery of the Mir Space Station generated by the engineering and science communities within NASA.

The general objectives of the Mir Photo/TV Survey are as follows:

- Study the effects of the space environment on a long-duration orbiting platform.
- Assess the overall condition of the Mir.
- Provide assurance of crew and Orbiter safety while in the proximity of the Mir Station.
- Understand the impact of plume impingement during proximity operations.
- Evaluate the equipment and procedures used to gather survey data.

The Image Science & Analysis Group (IS&AG) conducted several analysis tasks (based on user requirements) using the returned imagery data. They were to:

- Verify the configuration of the Mir complex.
- Assess the effect of micrometeoroid impacts and other visible damage on Mir surfaces.
- Document the condition of the docking mechanism.
- Analyze the effect of Shuttle and Mir RCS thruster firings on the Mir complex during different phases of the rendezvous.
- Measure the motion of Mir solar arrays during the Shuttle Primary Reaction Control System (PRCS) test.
- Characterize debris seen during and after docking operations.

- Determine the usefulness of image data in calculating approach and backaway velocities.
- Survey the newly installed Docking Module.
- Assess the quality of video and photographic data.

1.2 Summary of Findings

A summary of findings from each of the aforementioned analysis tasks follows.

1.2.1 Mir Configuration

Configuration information is important for proximity operations requiring visual navigation and for conducting loads simulations of docked configurations. Documentation of the Mir Station was compared to photography acquired during the rendezvous. The fly-around view in Figure 1-A identifies different Mir modules photographed during STS-74.

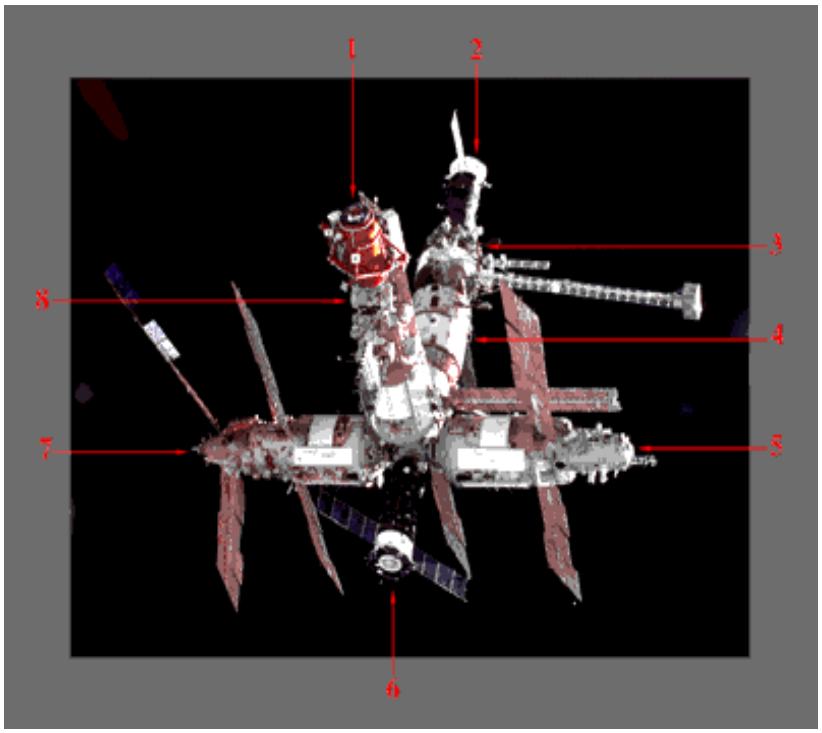

Figure 1-A Fly-around View of Mir Station

1. **Docking Module**
2. **Progress**
3. **Kvant**
4. **Base Block**
5. **Kvant-2**
6. **Soyuz**
7. **Spektr**
8. **Kristall**

1.2.2 Mir Surface Assessment

The purpose of the Mir surface assessment is to study the effects of the space environment on Station materials. This survey included analysis of all visible module and solar array surfaces. Starting with the Kvant SP#2 array, imagery acquired during STS-71 suggested that the surface of individual cells of the array (which had been on the ($+X_B$) side of Kristall prior to STS-71) may have been peeling off. Views from the back of this array captured during STS-74 revealed areas where entire strips of cells are lifted away from their underlying mesh support structure. The damage to this array does not appear to have been caused by micrometeoroid impacts since there are no broken edges on the cells themselves or noticeable damage to the underlying structure. A close-up view of the Spektr radiator facing the Orbiter provided excellent coverage of the blistering and chipping paint on the surface of the radiator. Similar to the Kvant array, this damage does not appear to be caused by micrometeoroid impacts since blistering would suggest other environmental causes. Areas of discoloration were found on surfaces of the Base Block, Kvant, and Spektr which had not been seen before. There are individual solar cells on the Base Block SP#2 and Kvant-2 SP#2 arrays which appear to be damaged. Figures 1-B and 1-C document the extent of detailed and overview coverage of the Mir Station acquired during STS-74.

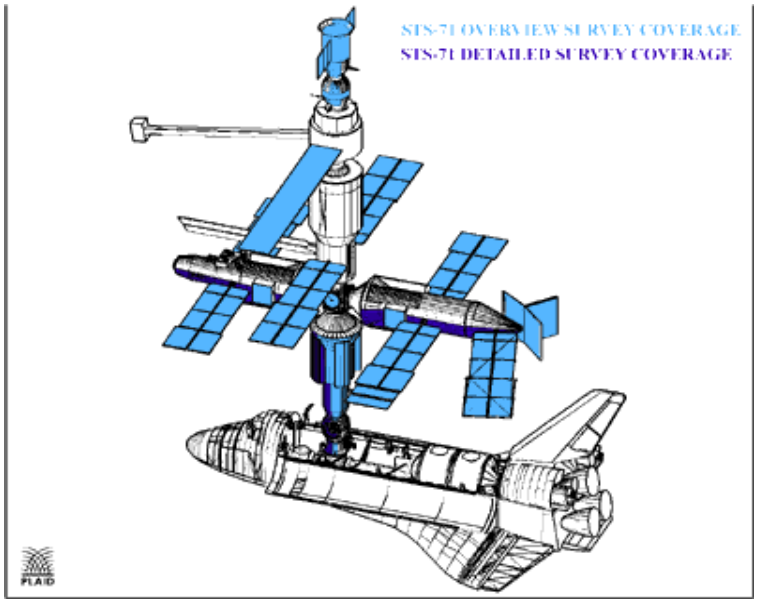

Figure 1-B STS-71 Mir Survey Coverage (Top View)

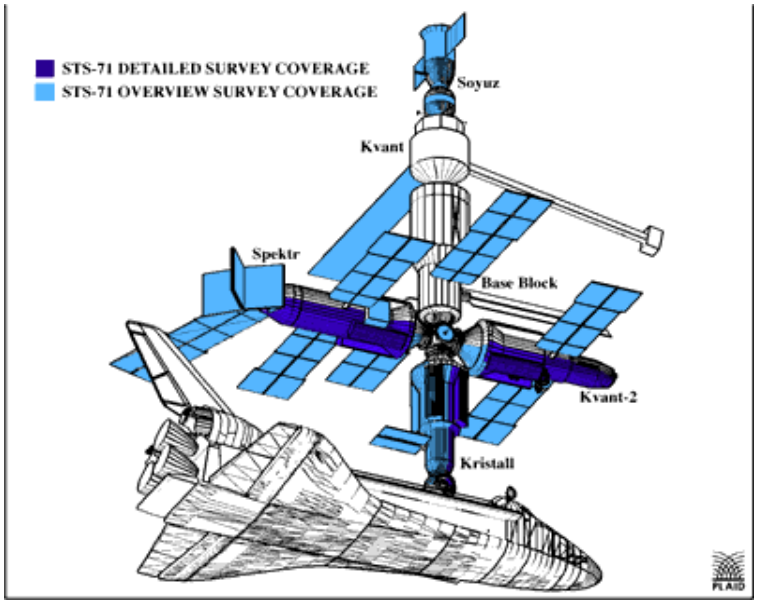

Figure 1-C STS-71 Mir Survey Coverage (Bottom View)

1.2.3 Docking Mechanism Assessment

An overall assessment of the docking mechanism and accompanying targets is made on each rendezvous mission. Both video footage and photographic data were acquired of the docking mechanism and target before and after the rendezvous. Views of the target revealed several areas on the backplate with surface material peeling. A comparison of available video and photographic views is presented. In general, ESC imagery showed the mechanism area and latch assemblies appeared to be free of damage and in good condition during backaway. In general, the mechanism area and latch assemblies appeared to be free of damage and in good condition from ESC imagery taken during backaway.

1.2.4 Solar Array Motion

Analysis of unanticipated motion of solar arrays is important for several reasons: concern about clearances during docking operations, verifying computer simulations of thruster plumes, and understanding how different array structures respond to those plumes. No array motion was visible during the approach phase. However, motion of Kvant-2 (8 inches peak-to-peak) and Spektr (2 inches peak-to-peak) solar arrays could be seen five minutes after docking. In addition, the Base Block array located directly above payload bay camera A appeared to oscillate (3 inches peak-to-peak) during rotation. Also, during the early part of fly-around, the Kvant array could be seen flexing approximately 24 inches.

1.2.5 Primary Reaction Control System Test Video Analysis

Although three identical Primary Reaction Control System (PRCS) tests were conducted on STS-74, only one had complete video coverage. Video of a Kvant-2 array was acquired while PRCS jets were fired during the docked phase. Motion and frequency analyses were

performed on the available test data and are included in Section 6. Results of this effort can be correlated with both the Photogrammetric Appendage Structural Dynamics Experiment (PASDE) results as well as accelerometer data gathered from the Mir Station.

1.2.6 Motion Analysis from Video

Payload bay camera video data was used to measure motion. During approach and backaway procedures, the Trajectory Control System (TCS) was used to determine distances from the Orbiter to the Mir Station. As on STS-71, the trajectory data was compared to calculations made from photogrammetric analysis of video data. Errors resulting from the video analysis were on the order of +/- 5 percent. This comparison will help future motion analyses when only imagery sources are available.

1.2.7 Debris During Docking Procedure

Several pieces of debris were seen during the time leading up to and after docking. While some of these objects can be attributed to backlit propellant, several of these particles appeared to originate from the payload bay and travel toward the Mir Station. Debris seen during a thirty minute interval around docking was analyzed. IMAX footage of the rendezvous revealed a button-shaped piece of debris bouncing around the payload bay after docking. However, no conclusive determination could be made on whether any of the visible debris might have made contact with Station surfaces. The velocity ranges of the different debris were between 1 inch per second and 18 inches per second. Debris sizes ranged from less than 0.5 inches to 2 inches.

1.2.8 Imagery Evaluation

STS-74 image data and acquisition procedures were evaluated. This mission marked the second time that the Electronic Still Camera (ESC) was available for DTO-1118 image acquisition. Assessment of image data is being performed to identify problems with procedures and equipment for subsequent rendezvous missions. Good coverage of Station surfaces was obtained for most rendezvous events except for backaway, when still photography was limited to ESC imagery.

Photo and video image sources are located in Appendix I.

2. MIR CONFIGURATION

A detailed assessment of the STS-74 configuration is presented. This involved identifying and labeling features directly from the photography. A comparison of expected and actual Station elements revealed features that were not identified in the documentation. These features are labeled as 'unknown' in the following images and will be discussed with Russian investigators.

Figure 2 shows the Mir Station as it appeared during the STS-74 approach.

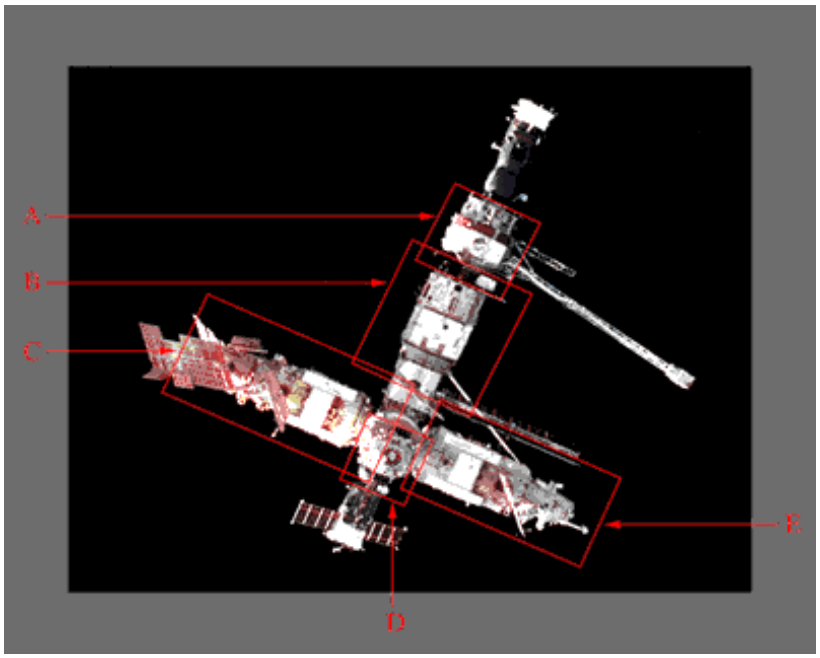

Figure 2 Mir Station during Approach

The boxes labeled A-E encompass regions whose exterior surfaces are described in detail within this section. Kvant (A) is an astrophysics and attitude control module. The Base Block (B) is the core module of the Station and provides habitation, power, thermal control and life support. The Spektr module (C) is used to study the Earth's environment and atmosphere. Figure 2-D shows the Docking Module (not seen in the above approach image) attached to the Kristall. Kristall (D) is used for material processing, remote sensing, and vehicle docking. Kvant-2 (E) supports extravehicular and remote sensing activities.

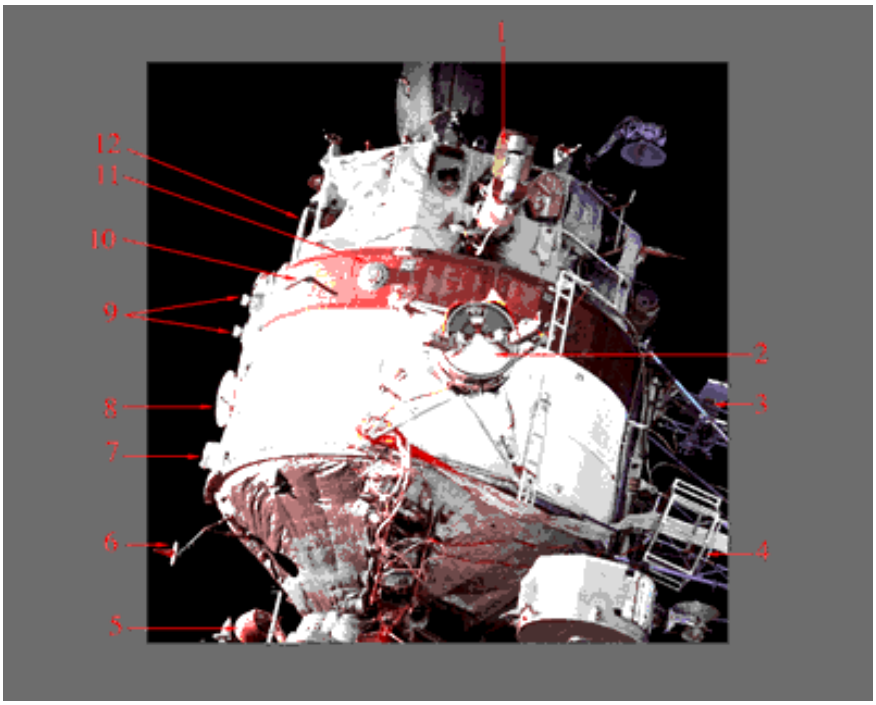

Figure 2-A Kvant

1. **Astrosensor**
2. **Solar Array Attach Port**
3. ***Unknown***
4. **Sofora Truss**
5. **Approach & Rendezvous Antenna**
6. **Igla Antenna**
7. **Instrument for Visual Orientation on Stars**
8. **Window Cover**
9. **Horizon Sensors**
10. **Radio Communication Antenna**
11. **Infrared Sensor**
12. **“Glazar” Telescope (edge-on view)**

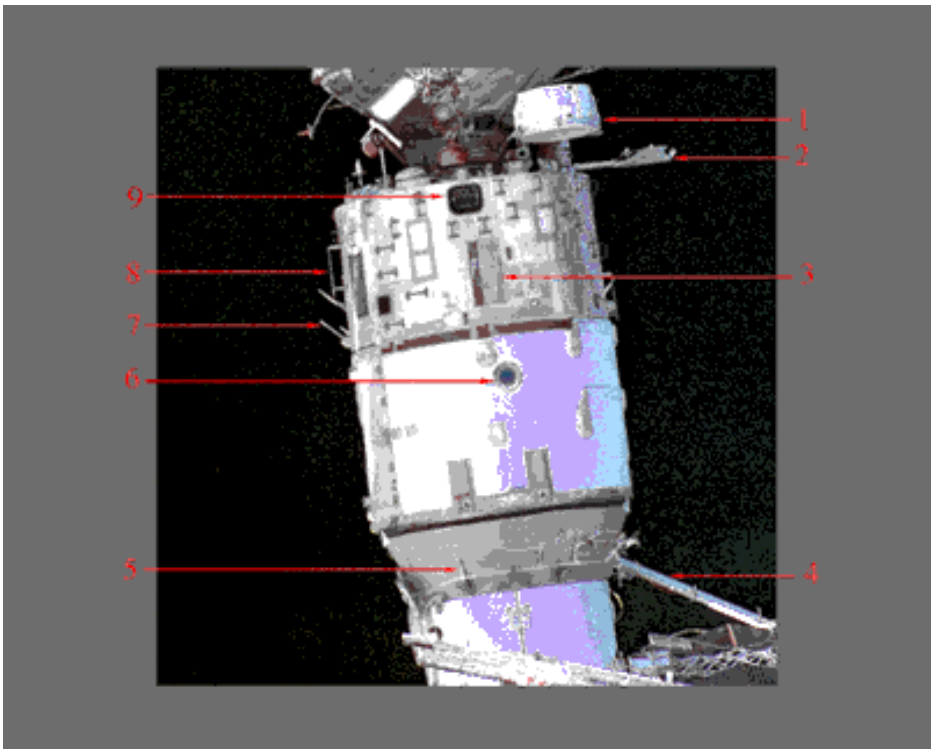

Figure 2-B Mir Base Block

1. **Luch Antenna**
2. **Approach & Rendezvous Antenna**
3. **Micrometeoroid Impact Sensor**
4. **“Strehla” EVA Transfer Aid**
5. **EVA Handrails**
6. **Radio Communications Antenna**
7. **EVA Handrails**
8. **Attitude Control Thrusters**

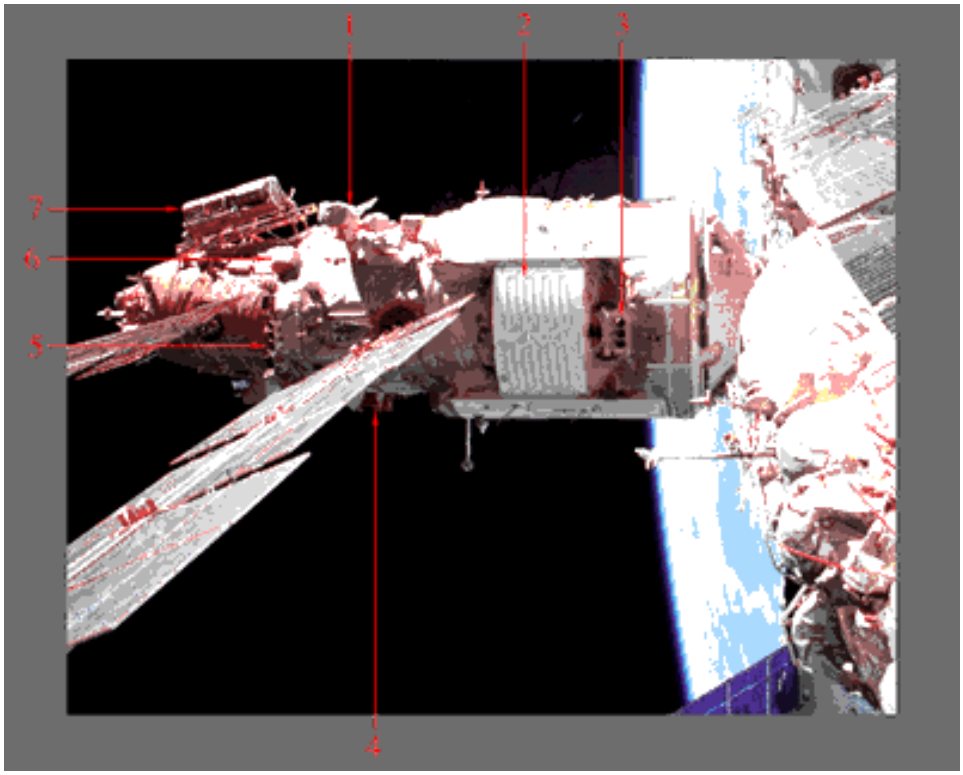

Figure 2-C Spektr

1. ***Unknown***
2. **Radiator**
3. **Precision Attitude Control Thrusters**
4. **Payload Pointing System**
5. **Attitude Control & Docking Thrusters**
6. ***Unknown***
7. ***Unknown***

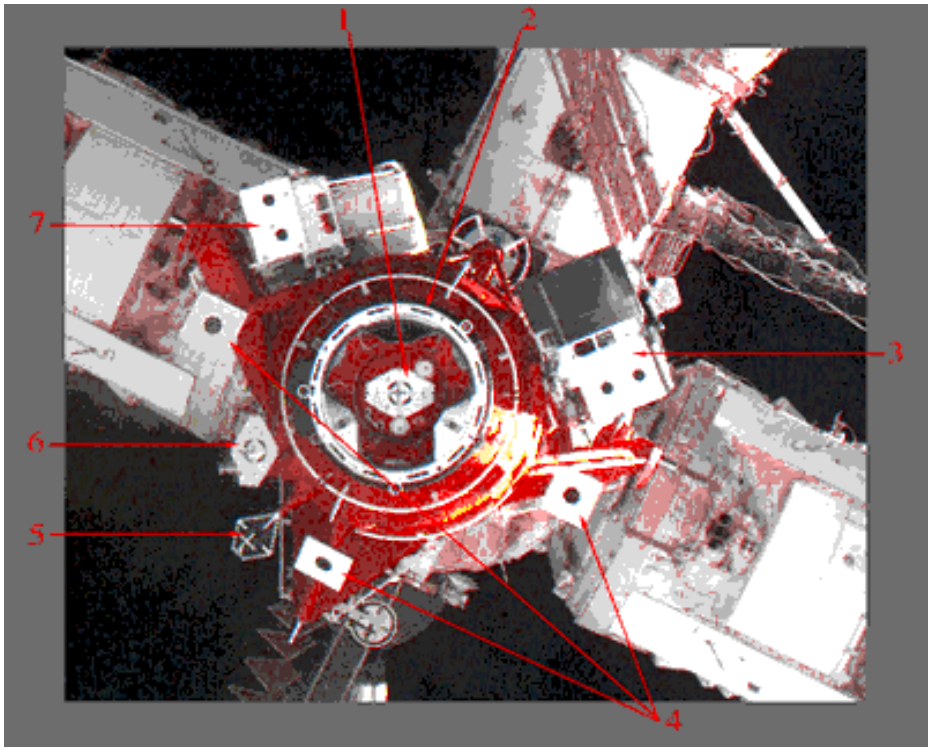

Figure 2-D Docking Module during Backaway

1. **New Docking Target**
2. **Structural Latch**
3. **Cooperative Solar Array (CSA)**
4. **Orbiter Space Vision System (OSVS) Targets**
5. **Soyuz Target**
6. **Docking Module Non Axial Target**
7. **Russian Solar Array (RSA)**

Survey imagery of the newly installed Docking Module is included in Appendix F.

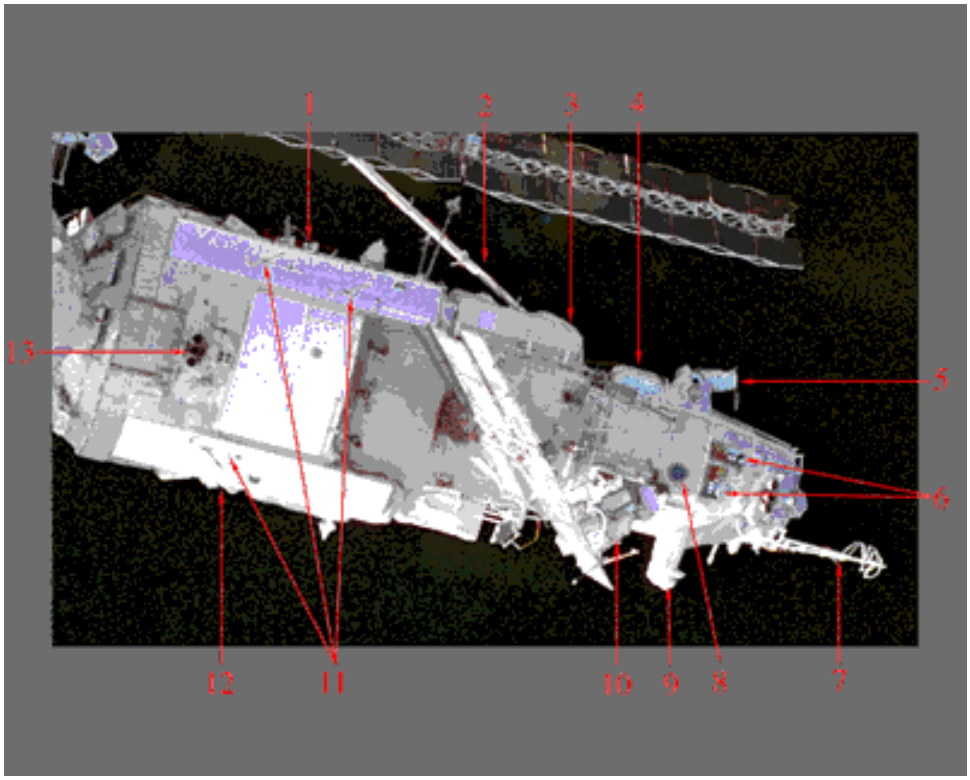

Figure 2-E Kvant-2

1. **Solar Sensor**
2. **“Strehla” EVA Transfer Aid**
3. **“Rodnik” Water Supply**
4. **Air Supply**
5. **Star Orientation Sensor**
6. ***Unknown***
7. **EVA Rails / Materials Exposure Platform**
8. **Window**
9. **Infrared Orientation Device**
10. **Television Camera**
11. **Antennas**
12. **Earth Orientation Infrared Sensor**
13. **Attitude Control Engines**

3. MIR SURVEY COVERAGE AND SURFACE ASSESSMENT

A survey of the visible Mir station components was performed to identify areas of damage and discoloration. Areas of damage were measured where possible using photogrammetric procedures on digital images that were scanned from film. Appendix A contains a list of the visible damage and discoloration found in this survey imagery. In addition, the list serves as a cross-reference for areas of interest that were seen during STS-63 and/or STS-71. The following diagrams present an overview of the damage and discoloration found from imagery collected on STS-74. Detailed images and descriptions of these damaged and discolored regions are given on the following pages.

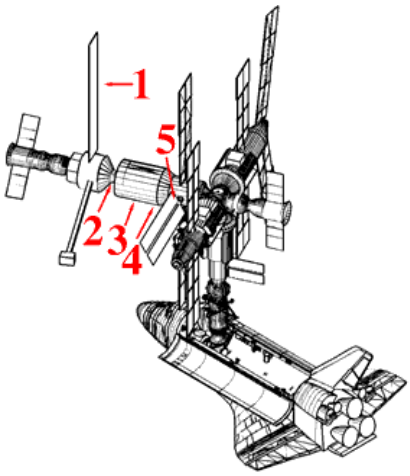

Figure 3-A STS-74 Damage Survey (Bottom View)

1. Kvant-2 bowed panel with surface damage.
2. Soyuz thermal blanket torn.
3. Kristall radiator with large area of discoloration.
4. SP#2 Base Block array with surface damage.
5. Spektr thermal blanket ablation.
6. Spektr radiator with chipped paint.

Figure 3-B STS-74 Damage Survey (Top View)

1. Kvant solar array.
2. Kvant fuel port probably creating splay pattern.
3. Base Block port window with chipped paint.
4. Base Block surface collar damage.
5. SP#3 Base Block array with missing

Figure 3-C is an image of the interface area between Kvant and the Base Block.

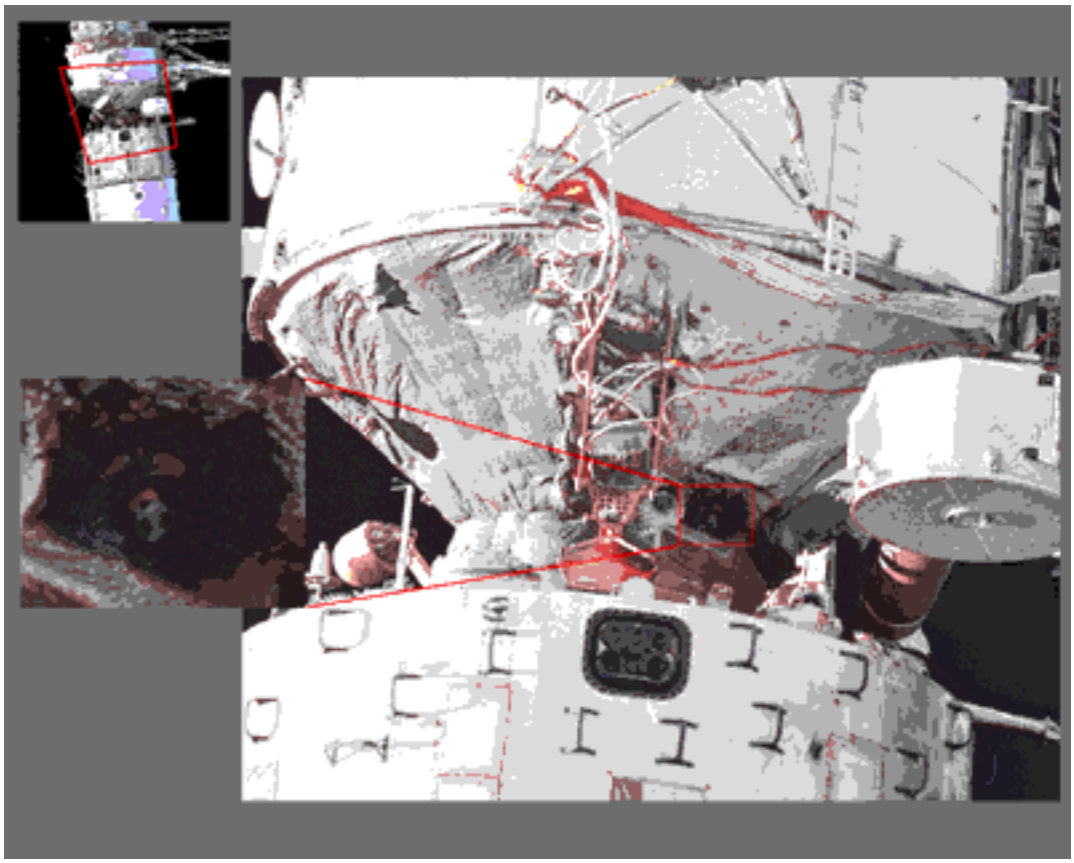

Figure 3-C Kvant / Base Block Interface Area

The fuel port on the end dome of Kvant (in the center of the highlighted box) could be one source of the splay pattern on the surface.

Figure 3-D is an image of the backside of the Kvant solar array. This array was previously installed on Kristall and was moved to Kvant between the STS-63 and STS-71 missions. This view was obtained through one of the Mir windows (probably from a window on Spektr). This damage was first seen on STS-71 imagery.

Figure 3-D Kvant Solar Array

The boxed area highlights a strip of cells which are partially detached from the solar panel. This same type of damage is also visible in at least 5 other areas of the array. In this particular region, there are four cells lifting up from the surface of the array with a total area of approximately 100 cm^2. (The size of one cell was measured to be 5 X 5 cm in the STS-63 report.)

The arrows suggest areas where further cells may be starting to detach since sunlight can be seen along their edges.

The combination of lighting from the front side of the panel and the image being captured from the back side of the panel highlighted this solar array damage.

This anomaly was not observed on STS-63 and may have occurred during relocation of the array from Kristall to Kvant.

Figure 3-E illustrates the prominent discoloration of Base Block surfaces. The surface of the Base Block photographed during STS-74 is at a 90 degree angle to that taken during STS-63. Non-blanketed areas are heavily discolored and appear to follow along the seams of adjacent panels. Similar discoloration was noted on STS-63 and STS-71 and appears to be uniform around the periphery.

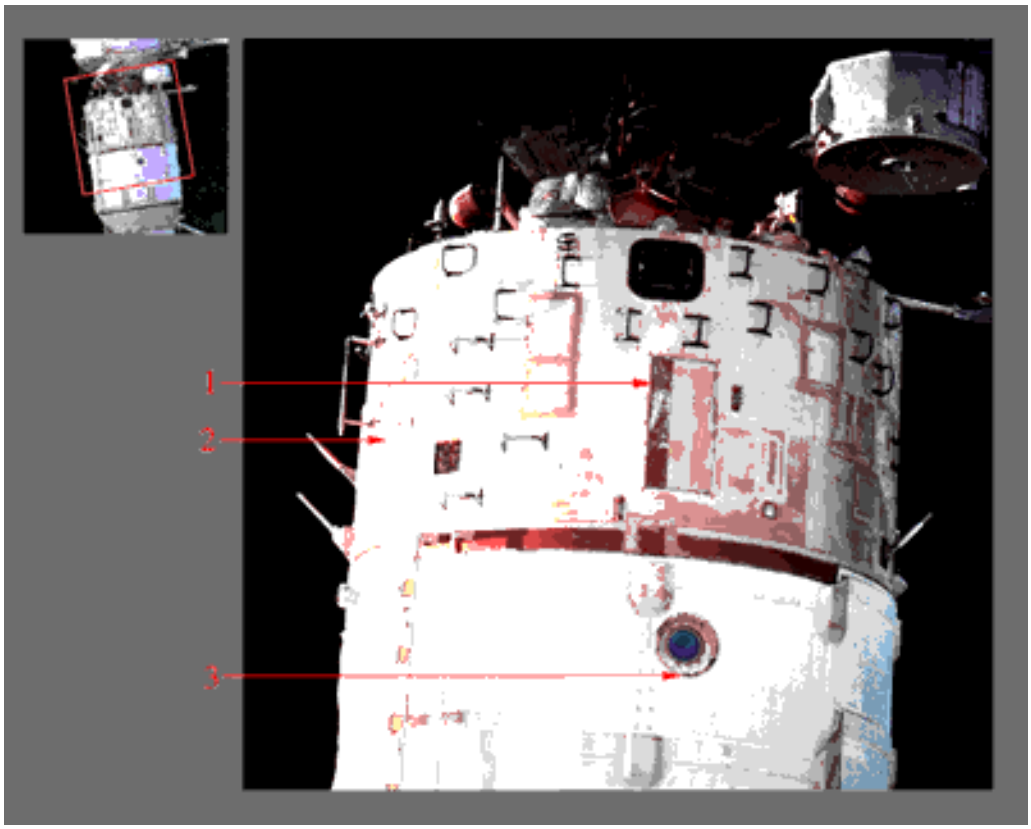

Figure 3-E Base Block Surfaces

There are a total of 4 micrometeoroid sensors around the circumference of the Base Block. Two micrometeoroid impact sensors are visible on the side of the Base Block which faced the Shuttle during the docked phase of STS-74.

Each of the three strips which appear to make up the micrometeoroid sensor were measured to be approximately 95 cm by 15 cm in the STS-63 report. One of these strips appears to be missing from the sensor in Item 1. The sensor pointed out in Item 2 was also visible during STS-63.

Item 3 points to a port window of the Base Block which has not been seen previously. The discoloration around the rivets securing the port window appears similar to discoloration seen around rivets securing the surface panels of the Base Block. In addition, several areas of paint around the outer edge of the window appear to be chipped off.

The outer edge of the window has areas of chipped paint and discoloration. Similar to rivets on surface panels, there seems to be discoloration around the rivets which secure the port window.

The following image takes advantage of lighting conditions where the sun is at an oblique angle to the surface being photographed.

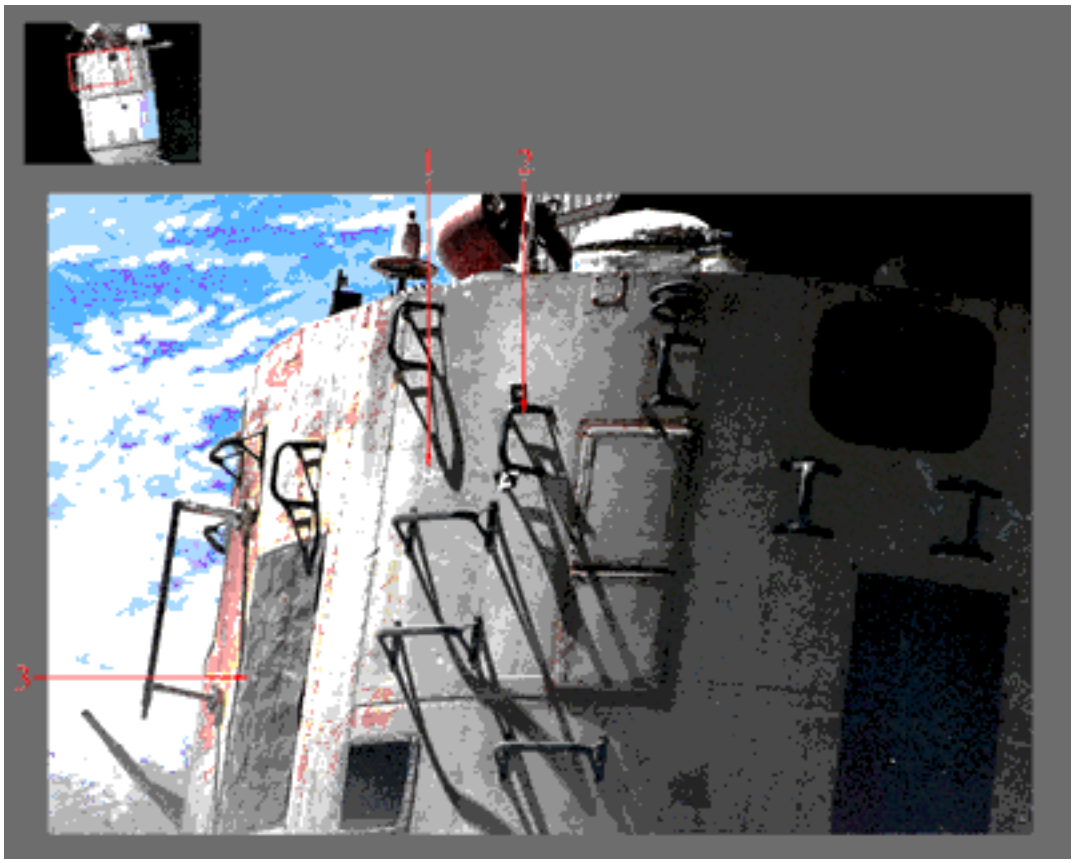

Figure 3-F Close-up of Upper Base Block

Item 1 is an area where apparently surface discoloration has been chipped away revealing a smooth “white” surface below.

Item 2 is an area where paint is blistering below an EVA handrail.

Item 3 is a micrometeoroid sensor. The effect of the oblique lighting angle provides a great deal of texture information on the uneven surface of the micrometeoroid sensor.

Figure 3-G shows discoloration and a piece of unknown material visible on the surface of the Base Block mid-section where the module diameter narrows. The white specks in the image are artifacts caused by dust and lint on the film during processing.

Figure 3-G Close-up of Base Block Mid-Section

Item 1 points to possible fibrous material sticking out along a seam between a surface collar and a panel of the Base Block. This area of unknown material was measured to be about 450 cm^2. This material is probably some type of thermal insulation.

Item 2 shows a region where discoloration on a Base Block surface collar appears to be scraped off, revealing a white surface below. Russian investigators have suggested that this may have occurred during Cosmonaut EVAs.

The general surface discoloration seen on this side of the base block appears similar to discoloration seen before around rivets and seams of adjacent panels on the other sides of the Base Block seen previously.

Figure 3-H is an image of the Base Block SP#2 array which extends out from the Base Block along the $-Z_B$ axis of the Mir Station. This array was oriented above the payload bay of the Shuttle during the docked phase of STS-74. This Nikon image appears to be taken from a window on the Base Block.

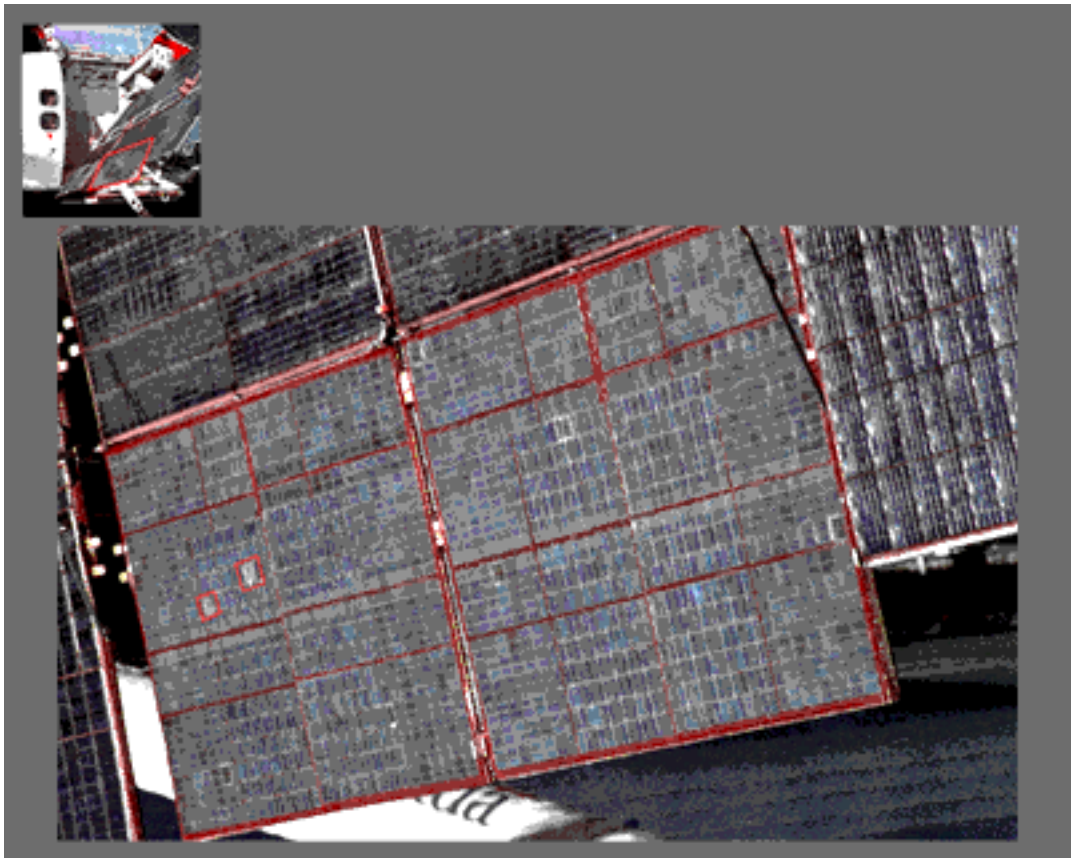

Figure 3-H Base Block SP#2 Array

The boxes point out areas where the surfaces of four solar array cells (two in each box) appear to be delaminated. The total damage area encompassed by the two boxes was measured to be approximately 16 cm^2.

Figure 3-I illustrates damage to the Base Block SP#3 array. This damage was first seen on fly-around imagery taken during STS-71. However, the fly-around imagery did not provide the detail of the image below.

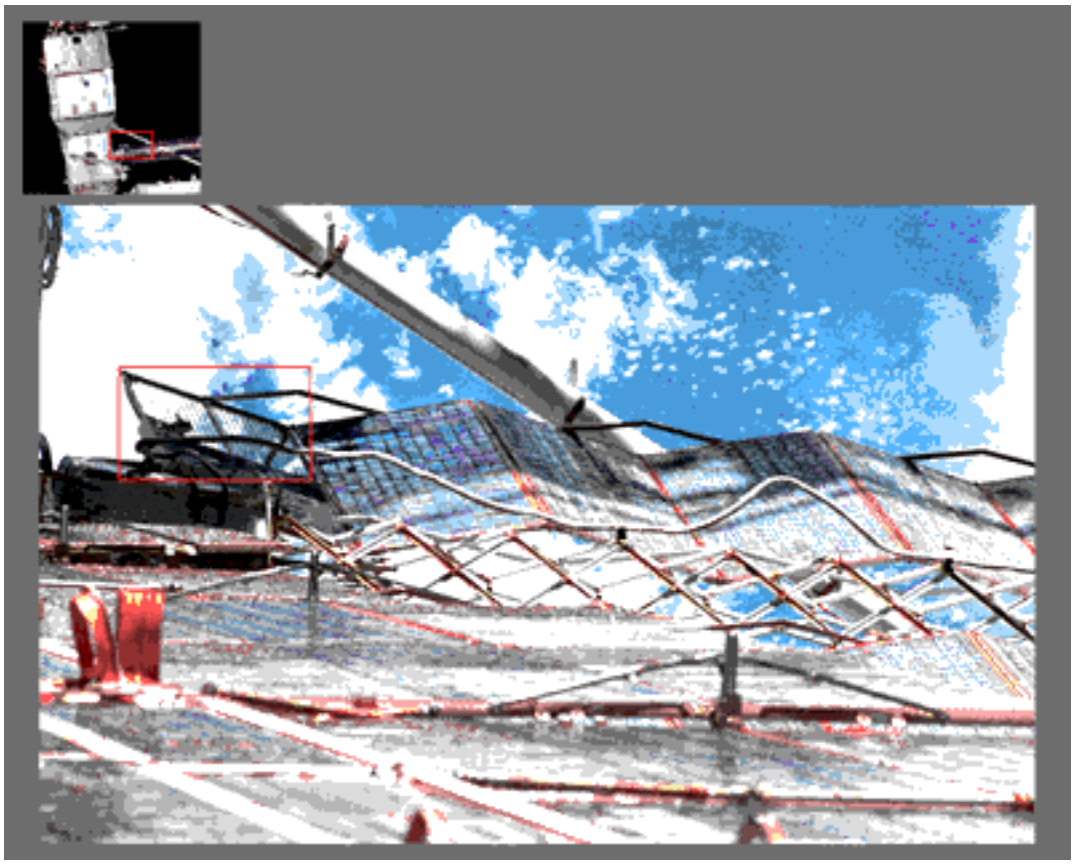

Figure 3-I Base Block SP#3 Array

The boxed area shows the region of the SP#3 array where a solar panel is missing near the array attach point on the Base Block. The missing panel was measured to be approximately 60 X 75 cm.

Figure 3-J shows the Kristall Docking Ring where the Docking Module was attached during STS-74. An open seam is just visible on the Soyuz thermal blanket at the left-hand side of the image. STS074-736-036 is a better image of this loose seam on the Soyuz blanket. A similar open seam was seen along a Soyuz blanket during STS-63.

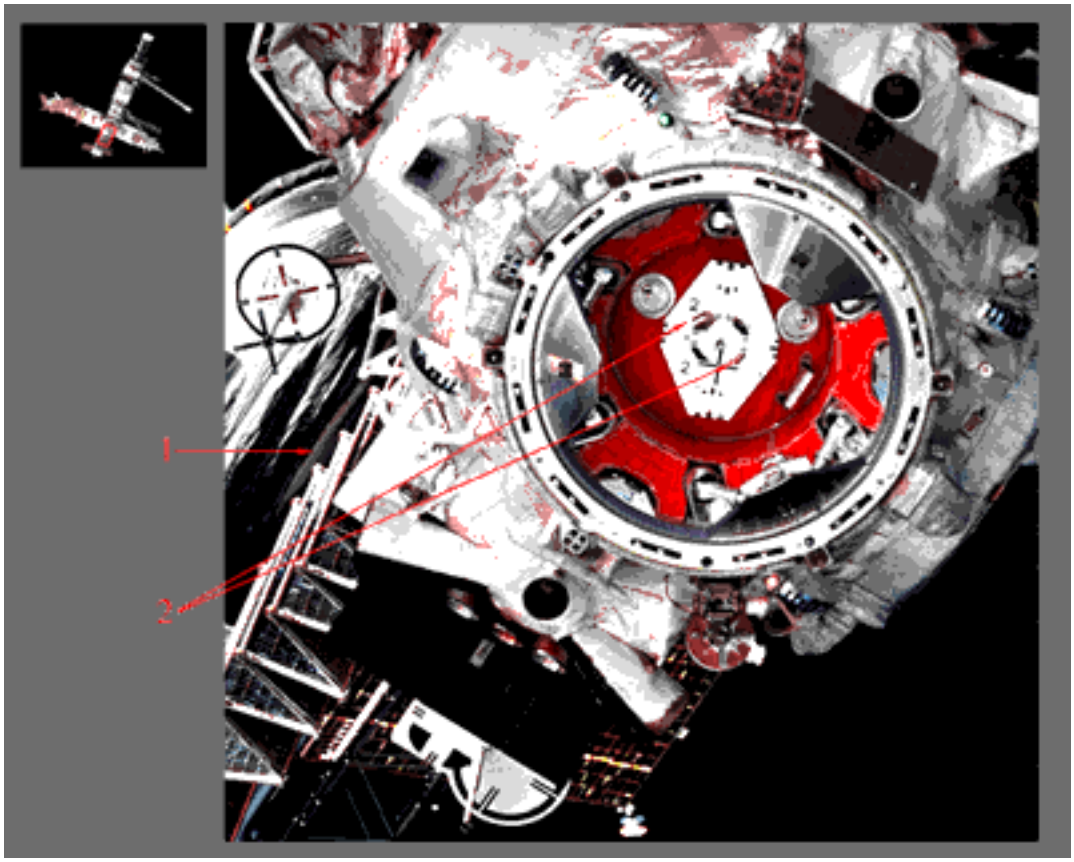

Figure 3-J Kristall Docking Ring

Item 1 points to what appears to be a seam along the Soyuz thermal blanket that has opened up.

Item 2 shows the paint peeling up from the surface of the docking target which was placed on Kristall during the STS-71 rendezvous. After only 4 months on-orbit, the target backplate showed significant peeling.

A discussion on the condition of the docking mechanism follows in section 4.

Figure 3-K shows discoloration surrounding the Mooring and Stabilization engines around the Kristall docking ring and missing material around the edge of the Buran target.

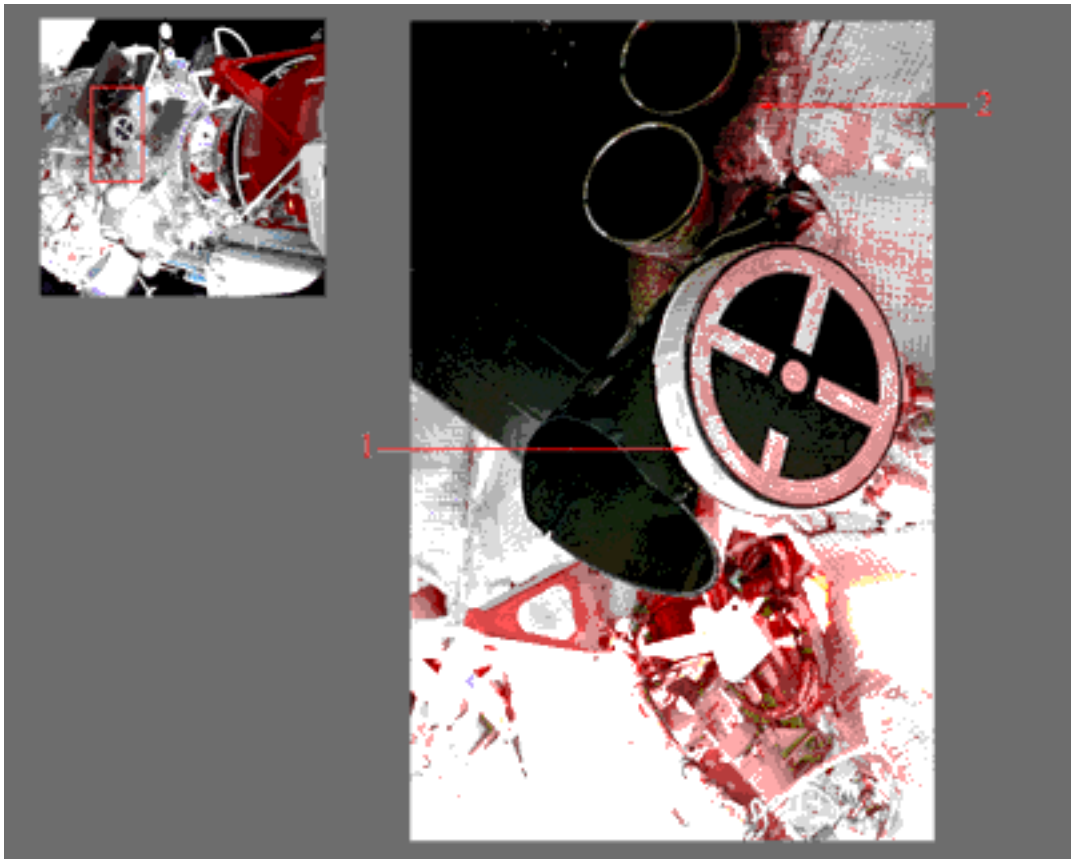

Figure 3-K Kristall Thrusters and TV Target

Item 1 points to a region around the edge of the Buran TV target where insulation appears to be missing. There may be more insulation missing around the edge of the target which is not visible in this image.

Item 2 shows the heavy discoloration of the thermal blanket surrounding the base of the attitude control thrusters.

Figure 3-L shows a close-up of the bowed panels on Kvant-2. This damage was seen on both missions STS-63 & STS-71.

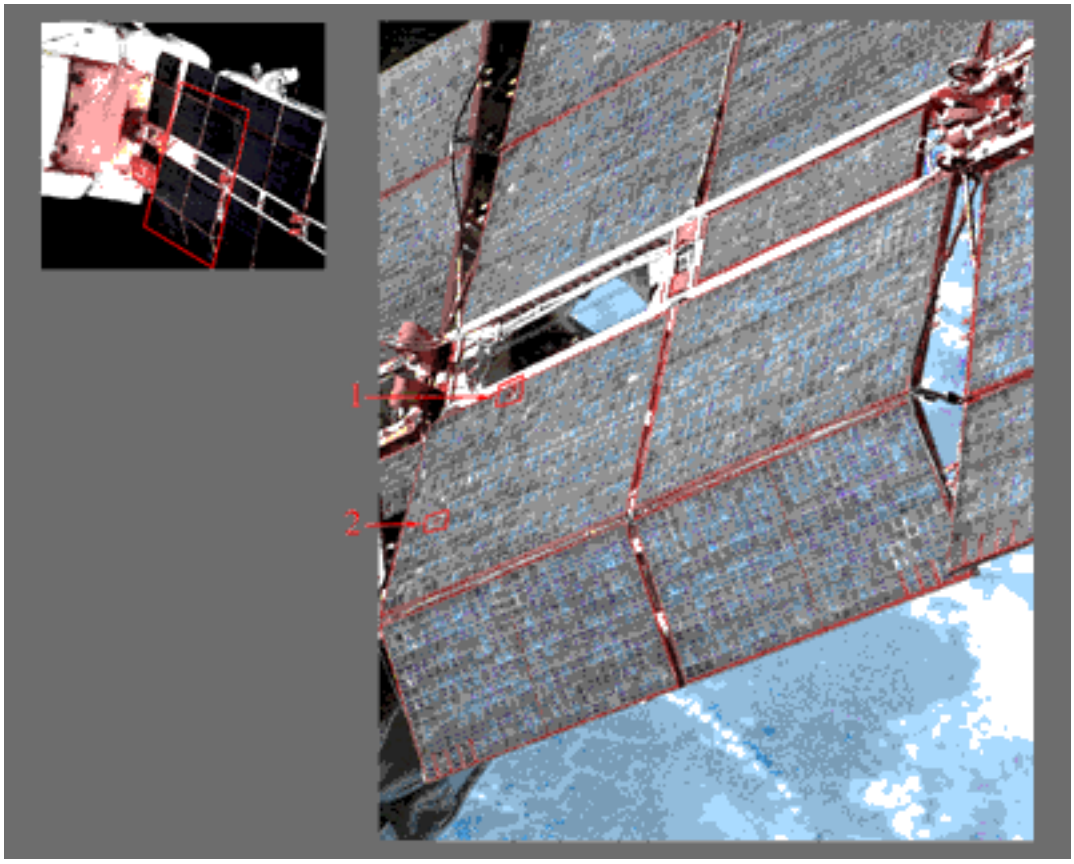

Figure 3-L Close-up of Kvant-2 Array #2

The bowed panel appears to have sustained damage to approximately 10 individual solar cells (Items 1 & 2). Due to the angle from which this image was taken, it is difficult to determine whether the damage was limited only to the top layer of cells.

The side of Spektr visible during the docked phase of STS-74 was rotated 90 degrees from that seen on STS-71. This provided an opportunity to gather baseline surface assessment information on this side of Spektr. Figure 3-M shows a radiator adjacent to the Spektr SP #2 array.

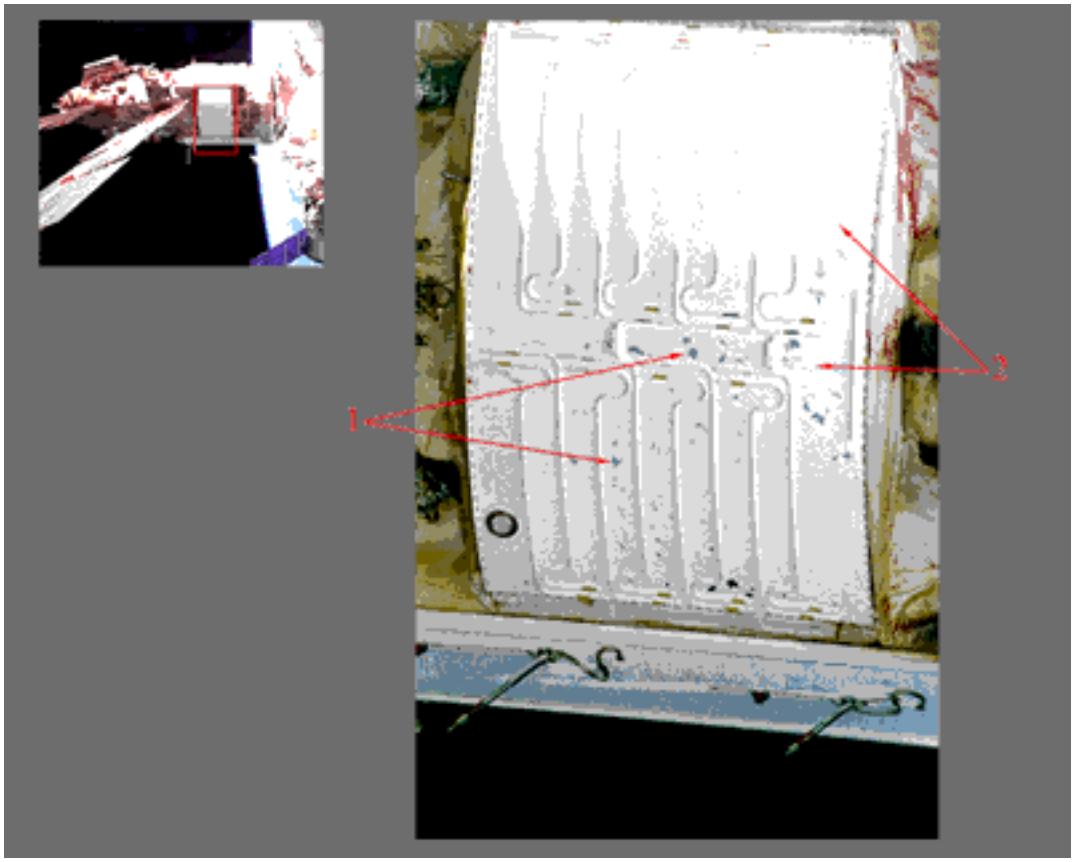

Figure 3-M Spektr Radiator

Over 50 areas of chipped paint are visible on the surface of the radiator. These chipped regions comprise an area of approximately 700 cm^2 which represents just over 1% of the surface area of the radiator.

Item 1 identifies two of the regions where paint has chipped off completely.

Item 2 identifies two of the regions where surface paint is blistering.

Some of the areas of chipped paint on the lower edge of the radiator were visible on photographs taken from an oblique angle on STS-71. This implies that the damage occurred either during the module's launch or between launch and STS-71. No close-out photography was available for comparison.

Figure 3-N shows discolored thermal blankets on Spektr between the damaged radiator and the docking node.

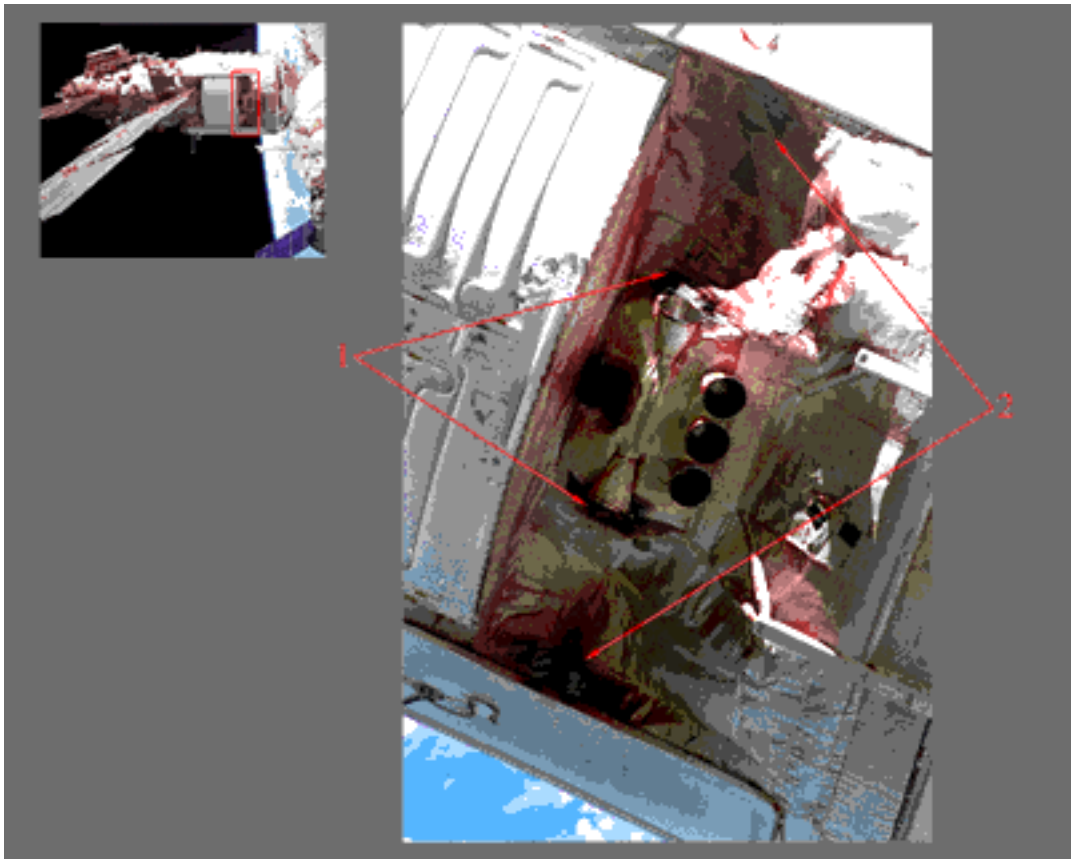

Figure 3-N Spektr Thrusters

Item 1 identifies darkened regions of the thermal blanket below the thruster nozzles. This discoloration may be caused by leaking propellant/lubricant.

Item 2 identifies areas of scorching and possible ablation to the thermal protection blanket caused by adjacent attitude control thrusters.

4. DOCKING MECHANISM ASSESSMENT

A survey of the docking mechanism was performed to verify its condition in preparation for STS-76. In addition, a target viewing assessment was conducted to evaluate the performance of the primary video camera (ODS centerline) used during the approach. This view was referenced to those seen on other available cameras. Analysis of these views could help in the determination of camera usage for ISS proximity operations.

Note that lighting conditions were good throughout much of the final approach phase.

4.1 Docking Mechanism Condition

Only a few Hasselblad (70 mm) photographs of the APDU were acquired. Much of the documentation of the docking mechanism during backaway relied on ESC photography. The structural latches, capture latches, body-mounted latches, alignment guides, laser retroreflectors, fluid/electrical socket/plug, and the centerline target all appeared to be in good condition on backaway based on the limited views available.

4.2 Target Visibility Comparison

Figures 4-A, B, C and D compare views of the docking area taken with two different video cameras and two different still cameras. Images of the mechanism and surrounding area were acquired using the Hasselblad (70mm) still camera, the ODS centerline video camera, and the elbow video camera during approach. The fourth image was acquired using the ESC during backaway. This comparison is intended to summarize views of the docking mechanism area obtained by the crew.

Only a few still photographs of the docking mechanism area during approach were acquired. Figure 4-A shows the best of these images. Section 3 of this report documented backing material peeling off the target backplate. This image was taken early on during approach with the Hasselblad (70mm) camera.

Since the primary function of the ODS centerline camera was to provide the crew with a means to visually align the target during approach, zoom settings were manipulated at their discretion. Damage to the target backplate surface is also visible on this view.

The camera on the RMS elbow was pointed at the interface area between the Orbiter and Station during the final moments of approach. This camera was used to acquire footage of the capture and transition between first contact and hard dock. Figure 4-C shows the Orbiter and Station interfaces just before docking. Small pieces of debris were visible around the interface are as the camera field-of-view zoomed in tighter.

Figure 4-D depicts one of the few available still images of the new Docking Module and associated targets during backaway. Note the OSVS targets surrounding the capture ring. This view also showed the bottom surfaces (identified with the double dot targets) of both

the Cooperative Solar Array (CSA) and the Russian Solar Array (RSA), both of which will eventually be installed onto the Kvant module.

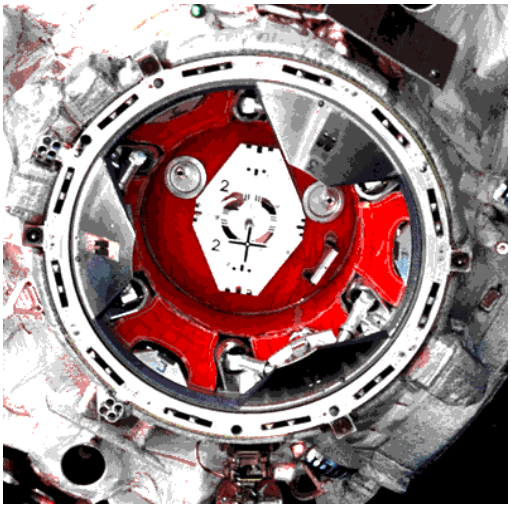

Figure 4-A Hasselblad (Approach)

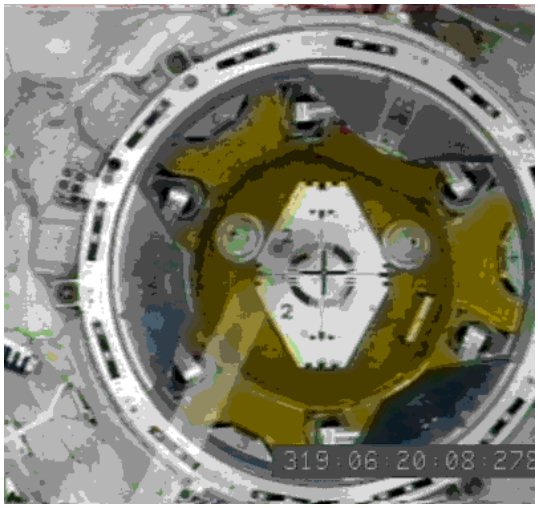

Figure 4-B Centerline (Approach)

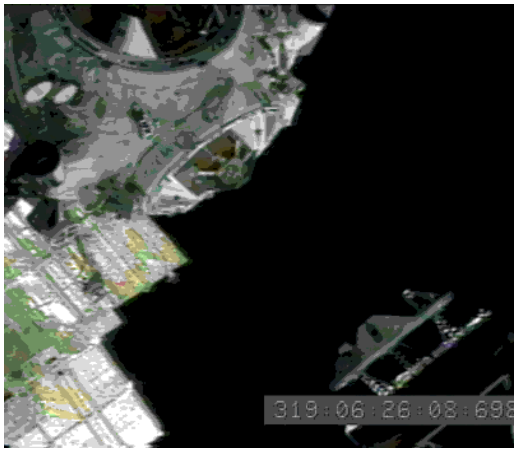

Figure 4-C RMS Elbow (Approach)

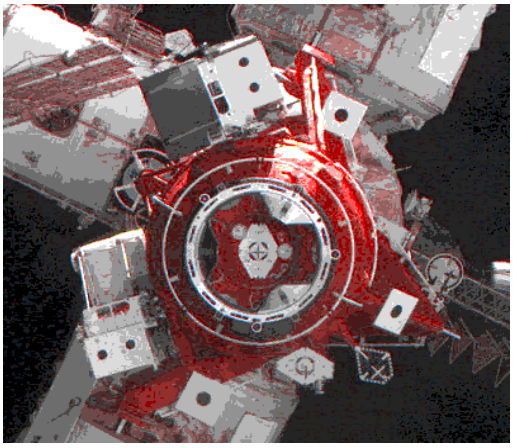

Figure 4-D ESC (Backaway)

5. SOLAR ARRAY MOTION

Unanticipated Mir solar array motion has now been seen on both docking missions. A unique event documented on this mission was the detection of array motion during the docked phase that did not appear correlated with plume impingement. Three different array motion events were noted while the Station was docked to the Orbiter. Kvant array motion was also noted during the early part of fly-around. Frequency plots and the tape ID numbers on which these motions were seen are included in Appendix D.

5.1 Kvant-2 / Spektr Array Motion while Docked

Substantial motion of the Kvant-2 SP#2 array was seen at 319:06:34:00 (approximately five minutes after docking). In addition, slight motion was also visible on the Spektr SP#2 array during this time.

The procedure to analyze the video data was as follows:

- Utilized an automated edge detection algorithm to track the motion of the Kvant-2 and Spektr SP#2 arrays' lower edges.
- Measured the amplitude of motion using features along the module surfaces as scaling factors and projecting those dimensions to the array edges.
- Input the data into a one-dimensional Fast Fourier Transform (FFT) to isolate specific frequencies.
- Interpreted the data to determine the existence of dominant frequencies.

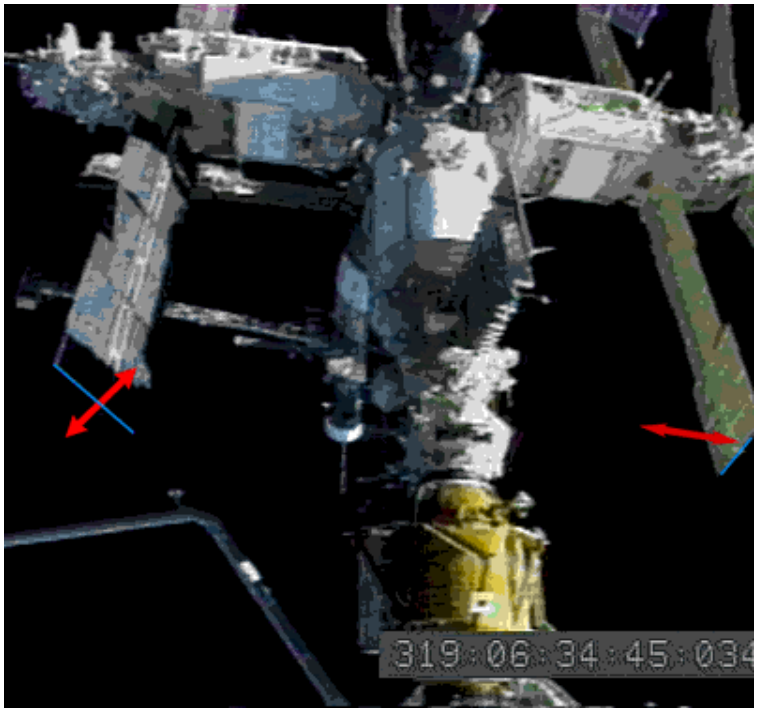

Figure 5-A Camera B View Showing Kvant-2 / Spektr Array Motion

Figure 5-A depicts the payload bay camera B view when the Kvant-2 SP#2 and Spektr SP#2 array motion was visible. Accompanying motion of the partially retracted SP#2 array on the Kristall module was evident by a change in the panel surface reflection. However, this latter motion was too difficult to quantify.

Figure 5-B shows motion of the two different arrays as a function of GMT time. The corresponding frequency of oscillation plots are contained in Appendix D. Analysis of this motion indicated a maximum peak-to-peak magnitude of about 7.5 inches for the Kvant-2 array and almost 2 inches for the Spektr array (+/- 0.5 in.), both with a dominant frequency of 0.2 Hertz.

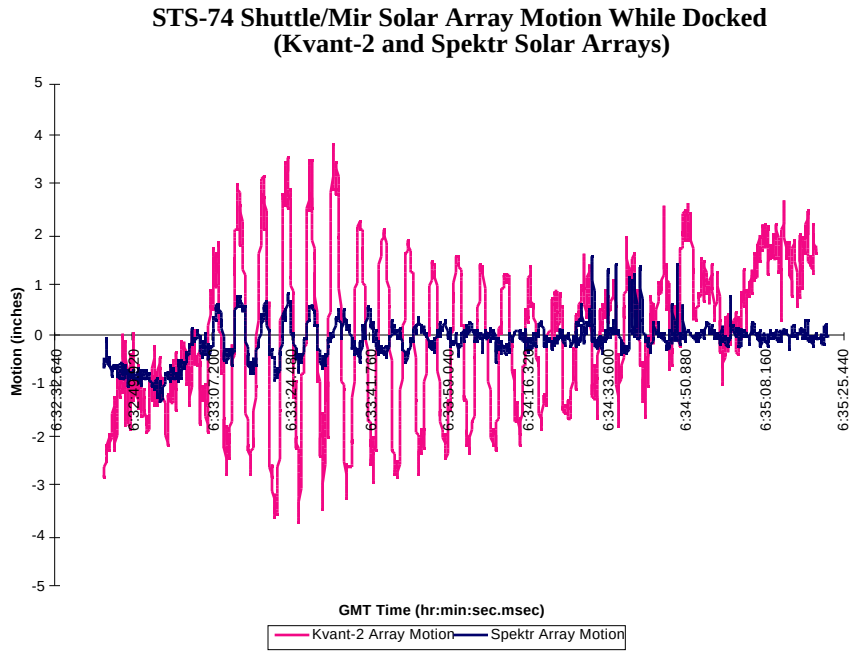

Figure 5-B Kvant-2 / Spektr Array Motion as a Function of GMT

Figure 5-B shows that the motion was visible for nearly two minutes. A common dominant frequency of oscillation is identifiable in the motion chart and was borne out in the frequency analysis. The existence of a lower frequency is suggested in the damped sinusoidal pattern, but none was identifiable in the frequency plot located in Appendix D.

5.2 Base Block Array Motion while Docked

Rotation of the Base Block SP#2 array was seen on a camera A view. An attempt to characterize this rotation was undertaken because the array appeared to oscillate at different times. Maximum amplitude of this oscillation was determined to be about 3 inches (+/- 0.5 inches). Several minutes after this rotation, the array was also seen to oscillate in a motion parallel to the array width. The maximum amplitude of the lateral motion was measured to be 5.5 inches. Detailed analysis could not be performed on this motion

because of problems in discriminating the array edge from the background. While no definitive sources for either of these motions were identified, discussions with Structures and Dynamics engineers suggest that they were *not* indicative of plume impingement.

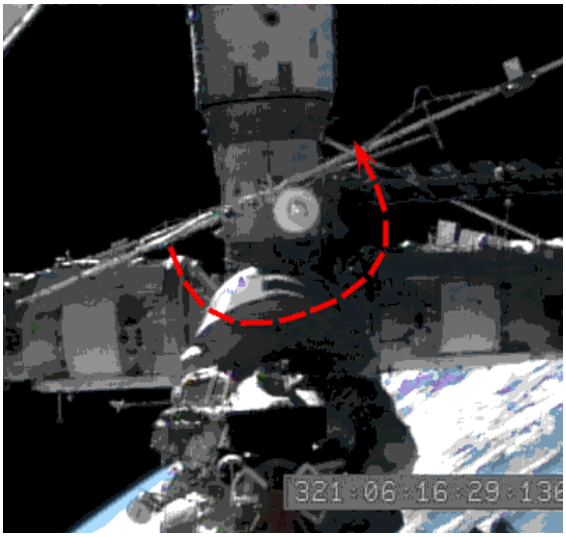

Figure 5-C Camera A View Showing Base Block Array Motion

Figure 5-C depicts the payload bay camera A field-of-view when the Base Block solar array rotation was visible. Figure 5-D shows this motion as a function of rotational position. The corresponding frequency of oscillation plot is contained in Appendix D.

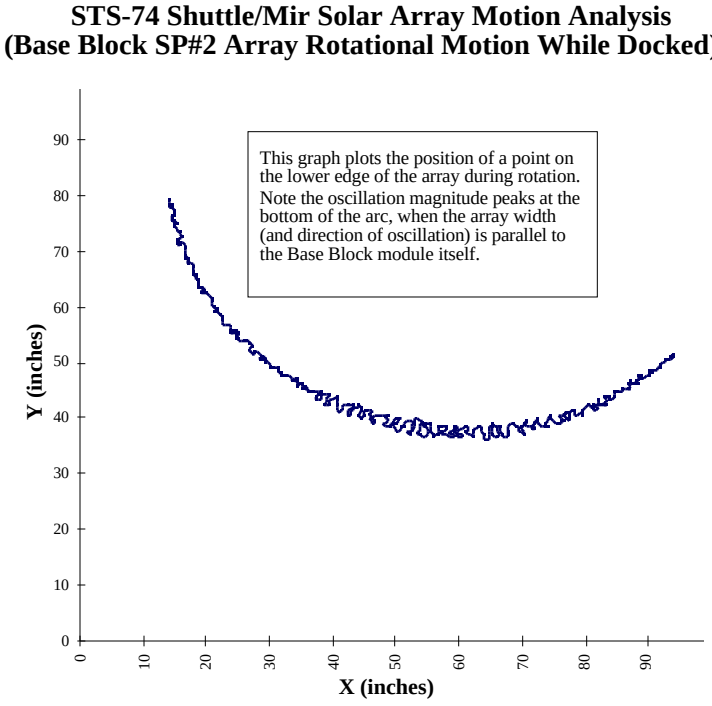

Figure 5-D Base Block Array Motion as a Function of Rotational Position

Figure 5-D shows the motion as a function of rotational position. The corresponding frequency plot generated by analyzing motion along both the x-axis and y-axis as a function of time is located in Appendix D. Peak frequencies were identified at 0.25, 0.30 and 0.35 hertz.

5.3 Kvant Array Motion During Fly-Around

Only one array motion event was seen outside the docked phase. The Kvant SP#1 array flexed during the early part of fly-around at 322:09:56:30. This motion was preceded by a visible sequence of firings from Progress and Base Block thrusters as identified in Figure 5-E. The sources and apparent direction of these firings are also plotted on the timeline in Figure 5-F.

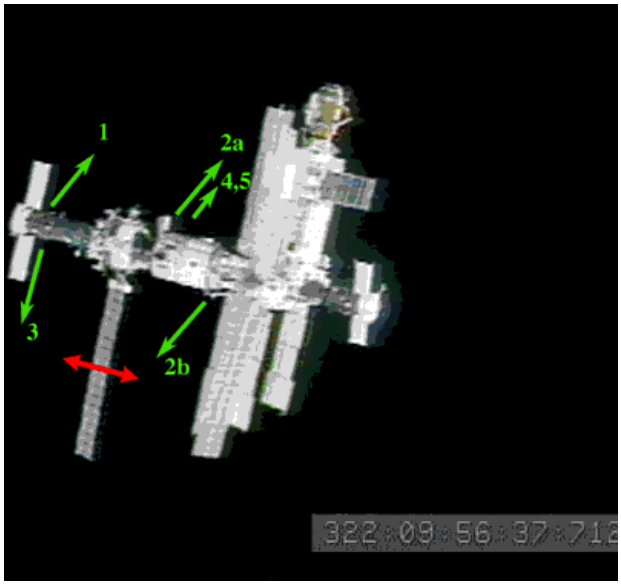

Figure 5-E Camera D View Showing Kvant Array Motion

Figure 5-E shows the camera D view used to document motion of the Kvant SP#1 array during fly-around. The orange arrow indicates maximum motion occurred at the center of the array. And unlike the other types of motion documented on this mission, the Kvant array appeared to flex, perhaps displaying torsion. Whether this motion could be attributed solely to plume impingement or by forces induced by Mir thruster firings could not be verified. The maximum peak-to-peak amplitude of motion was measured to be about 24 inches (+/- 6 inches). The error term is a function of the measurement accuracy of features that are a significant distance from the camera and only comprise a few pixels on the digitized video.

Figure 5-F characterizes the motion of the Kvant array after Mir thruster firings. There appeared to be three distinct oscillations of the array during the sequence. These oscillations may be the source of the lowest frequency peak of 0.065 hertz, with an additional peak noted at 0.65 hertz. Appendix D contains the frequency plot generated from this data.

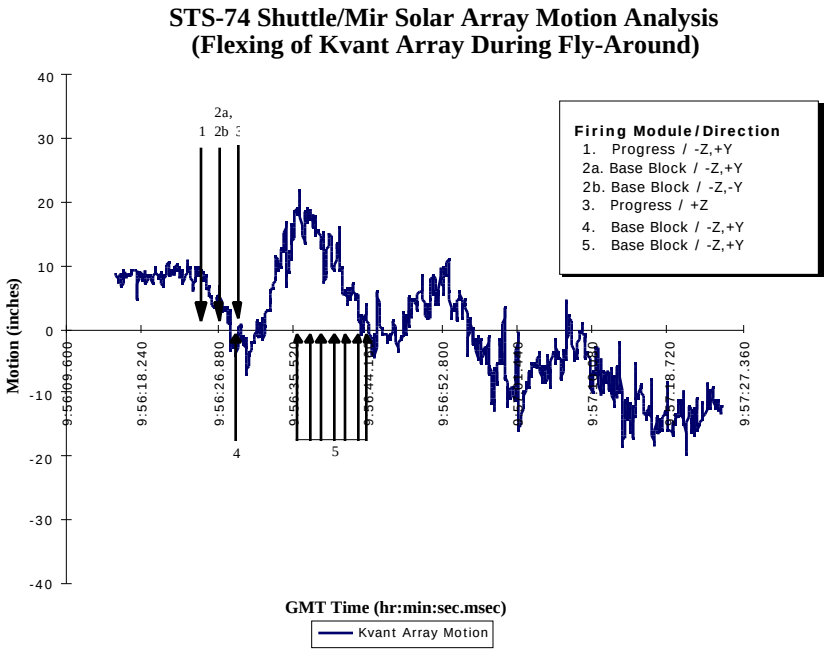

Figure 5-F Kvant Array Motion as a Function of GMT

Figure 5-F documents the array motion as a function of time. Mir thruster firings and their direction (in Mir coordinates) seen around the time of motion are included in the graph. Note that the documented firings are just those that were visible and are not necessarily comprehensive. The downward-pointing arrows on the graph denote major pulses from the specified thrusters. The smaller, upward-pointing arrows identify what appeared to be minor pulses that may have contributed to the motion. The corresponding frequency plot is located in Appendix D.

5.4 Solar Array Motion Error Analysis

The automated edge-tracking programs used in the analysis of array motion reduce conventional measurement errors to sub-pixel levels. Therefore, most of the errors generated in the calculations can be attributed to two sources: the inaccuracies of scaling factors at available video resolution, and assumptions about the relative orientation of Station features to the Orbiter.

6. PRCS APPENDAGE MOTION VIDEO ANALYSIS

Three identical Primary Reaction Control System (PRCS) tests were performed during the docked phase. Complete video coverage was only acquired on one: Open Loop Test 2. The goal of this test was to determine the effect of using Orbiter thrusters (normally used to control Shuttle/Mir movement) on Mir appendages. Video data was used to determine maximum amplitude of motion of the Kvant-2 SP#2 array. In addition, analysis was performed to verify the presence of dominant frequencies in the array motion. Motion and frequency plots generated from each sequence in Open Loop Test 2 are documented in Table 6-A. The procedure used in the analysis was similar to that described for the solar array motion analysis.

The accompanying image and plots are representative of the data and analysis performed. Frequency plots of each of the four sequences are located in Appendix E.

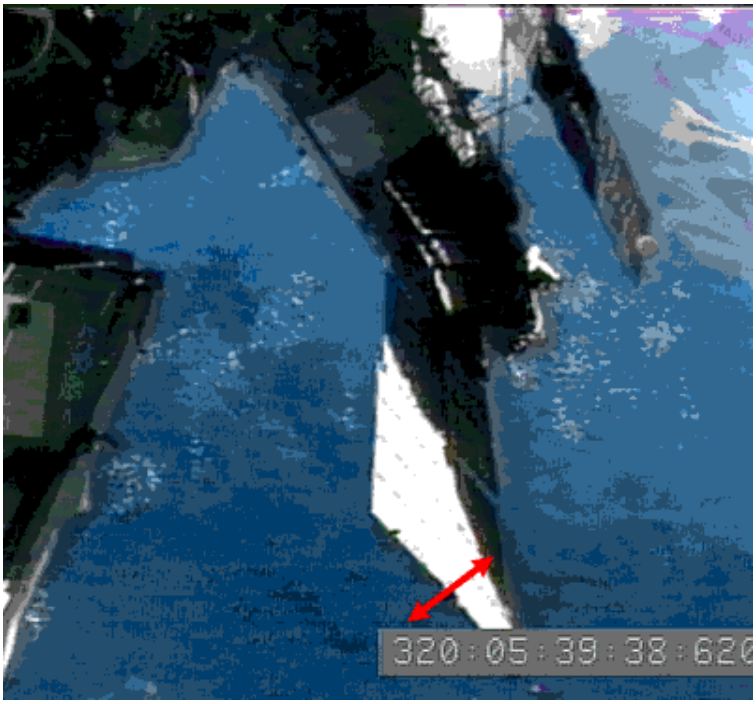

Figure 6-A Camera A View During PRCS Test

Figure 6-A shows a typical camera A view during the sequence of thruster firings in Open Loop Test #2. The field-of-view obtained for this test, while adequate for analysis, was wider than anticipated. Figures 6-B, 6-C, 6-D and 6-E are plots of the Kvant-2 SP#2 array motion as a function of GMT for each of the four tests.

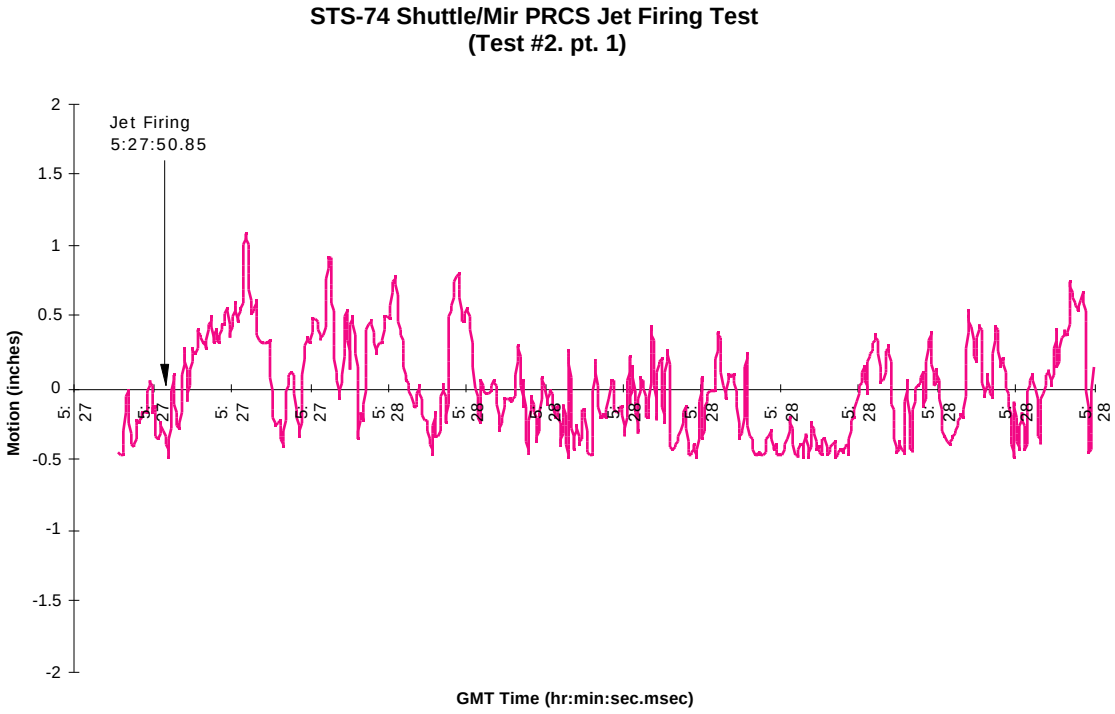

Figure 6-B PRCS Test Sequence 1 as a Function of GMT

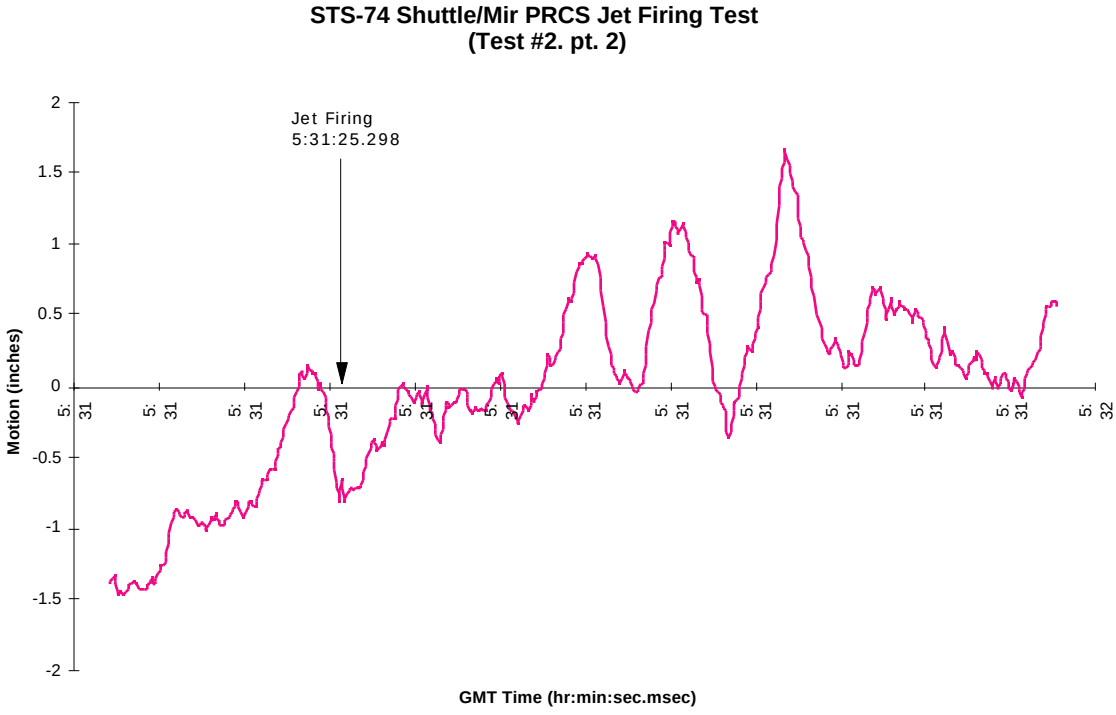

Figure 6-C PRCS Test Sequence 2 as a Function of GMT

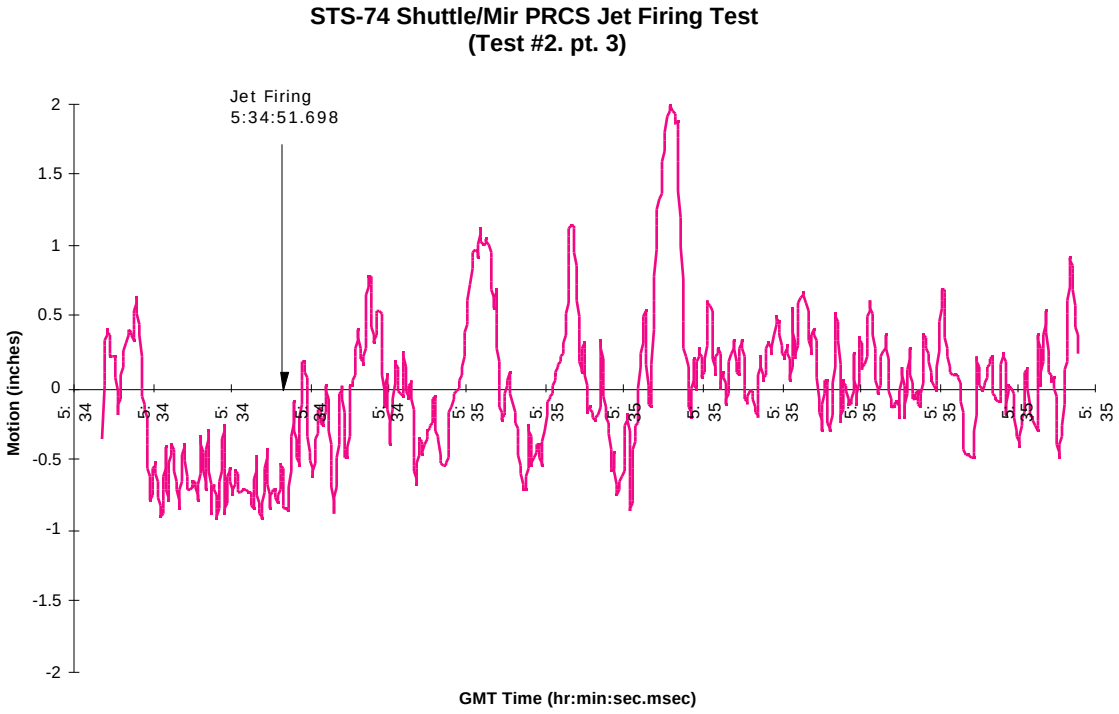

Figure 6-D PRCS Test Sequence 3 as a Function of GMT

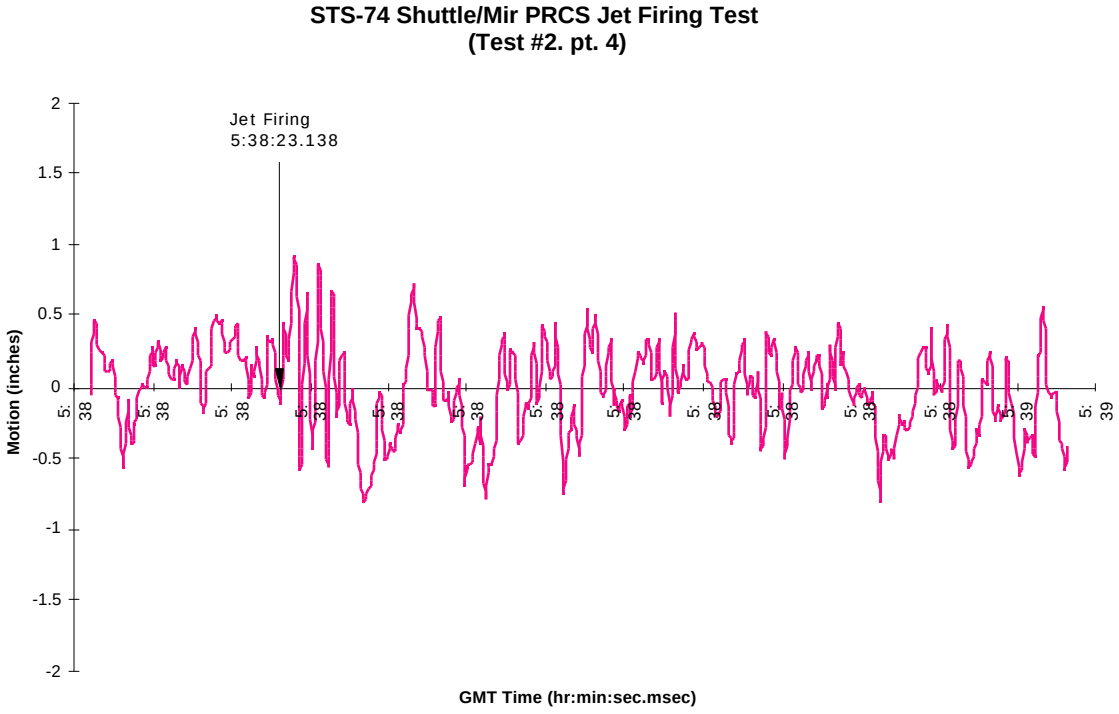

Figure 6-E PRCS Test Sequence 4 as a Function of GMT

All of the accompanying PRCS frequency plots are included in Appendix E. A summary of results obtained from analysis of the video test data is shown in Table 6-A.

Number	Pulse Duration / Direction of Motion	Shuttle RCS Jets	GMT Time	Max. Amplitude (inches)	Peak frequencies (Hertz)
1	**80 ms +Pitch**	F3D, F4D	320:05:27:50.858	1.5	0.30
2	**160 ms -Pitch**	L3D, R3D	320:05:31:25.298	2.0	0.20
3	**160 ms -Roll**	F3D	320:05:34:51.698	3.0	0.20
4	**160 ms -Yaw**	L1L	320:05:38:23.138	1.5	0.20

Table 6-A Analysis of PRCS Open Loop Test #2 Video Data

The maximum amplitude designation in Table 6-A was determined from the first major peak-to-peak motion after the specified thruster firings. The ability to achieve sub-pixel accuracies in the edge tracking algorithm imply that scaling factors were the primary source of error in the data. This error was on the order of +/- 0.5 inches for the motion results.

Dominant frequencies were derived in the interpretation of frequency-domain plots generated for each test. Some subjective judgment was made in the selection of peaks, since higher frequencies are often associated with noise in the data. Primary sources of error in the interpretation of this frequency data are the resolution of the output plot (+/-0.05 Hertz) and the resulting peak selection procedure.

A direct comparison of the amplitude results obtained from the STS-71 and STS-74 PRCS tests is not valid since the configurations were different for each mission. However, similarities may exist between corresponding frequency plots for common thruster firings.

Number	Direction of Motion	Shuttle RCS Jets	Max. Amplitude (in.		Peak frequencies (Hz)	
			STS-71	STS-74	STS-71	STS-74
1	+ Pitch	F3D, F4D	0.5	1.5	.075	0.30
2	- Pitch	L3D, R3D	0.5	2.0	.150	0.20

Table 6-B Comparison of PRCS Video Results from STS-71, STS-74

Table 6-B shows the two tests were the same pairs of jets were fired on both STS-71 and STS-74. Motion measurements were significantly different between the two missions. The peak frequency for the STS-74 +Pitch test was a multiple of the corresponding STS-71 test. The lack of correlation between the corresponding -Pitch tests could not be explained.

7. MOTION ANALYSIS FROM FILM AND VIDEO

Information extracted from recorded video was used to calculate distances from the Shuttle to the Mir during approach and backaway. This procedure is being studied to determine its usefulness for future motion analysis of known objects in space where trajectory control data may not be available. Trajectory Control System (TCS) data available during the rendezvous served as ground truth for the analysis.

Video and photographic coverage of the Mir during approach and backaway were reviewed for this analysis. Measurements were made from the video to determine relative motion between the Shuttle and Mir during these times. Uncertainties about lenses used during the approach and backaway procedures precluded the use of still photography for this comparison.

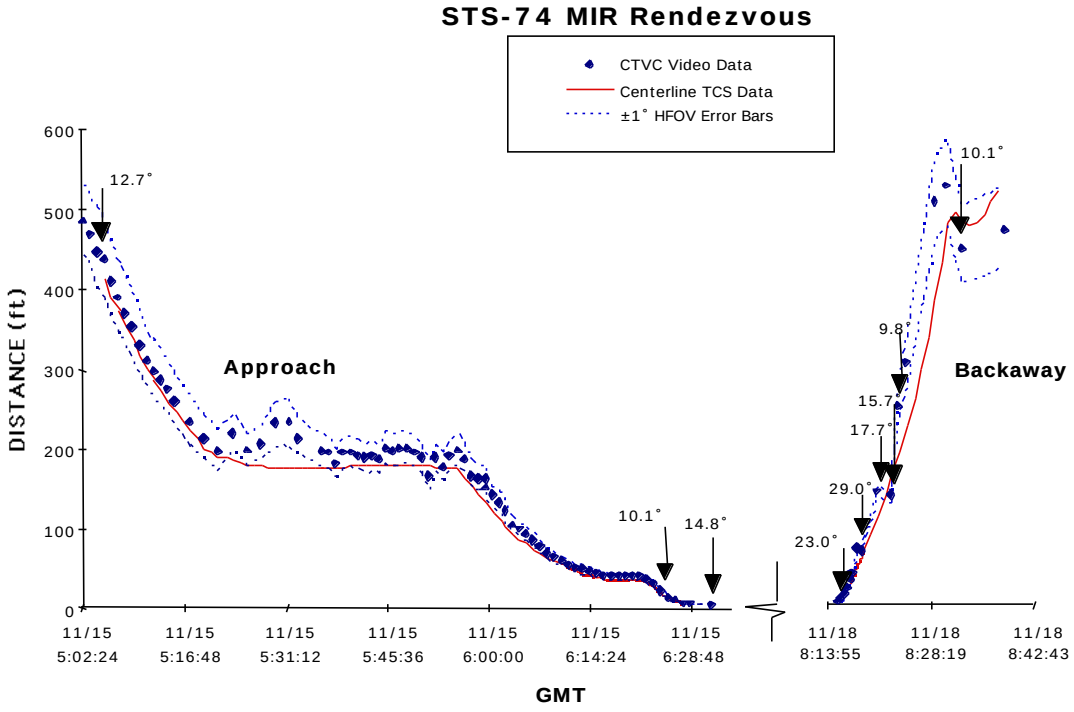

Figure 7-A Orbiter to Mir Distance Comparison using TCS and Video Data

Figure 7-A compares actual TCS data with CTVC video calculations. Horizontal-field-of-view (HFOV) information embedded in the vertical interval was used to calculate the separation distance between the Orbiter and the Mir. Each change in the HFOV is signified by an arrow in the graph above. These numbers have inherent errors of approximately +/- 1°, and when propagated through photogrammetric equations, result in the error bars shown in the figure. The errors were on the order of +/- 5 percent when the Orbiter and Station docking interfaces were parallel. Other errors were induced during transitions from one zoom setting to another. Centerline video was the primary source of data used in the analysis. However, payload bay camera C and D views were also incorporated during part of the backaway. A comparison with earlier rendezvous missions indicates refinement of the camera and scaling selection procedure have improved results.

8. DEBRIS SEEN DURING DOCKING OPERATIONS

Small pieces of debris can be seen on orbit during most missions. Docking Module installation activities in the payload bay may have contributed to some of the debris seen during STS-74. The timeline in Figure 8-A shows the different debris events seen during the docking procedure. Several pieces of debris were tracked and characterized and are considered representative of the more than 50 pieces seen around the time of docking. Velocity and size estimates were based on using Docking Module features as scaling factors.

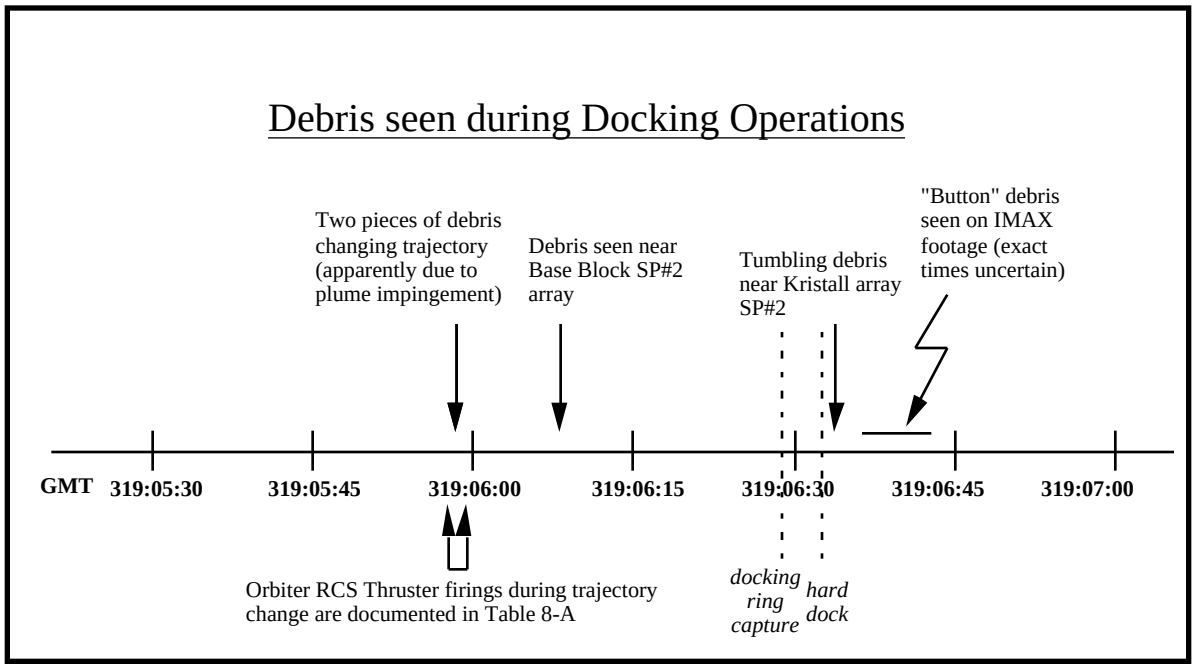

Figure 8-A Debris Timeline During Docking Operations

Figure 8-A documents the specific debris "events" which were characterized in this analysis. One cluster of debris (made more visible due to lighting conditions) was seen during a three minute interval starting approximately thirty minutes before soft dock. Thirty-two small pieces of light colored debris were noted between the Orbiter and the Mir Station. Two of these pieces were deflected from their initial trajectory by what appeared to be an interaction with unseen plumes. Ten minutes later, a zoomed-in view from camera B showed a piece of debris near the Base Block SP#2 array. Just after docking, nine small pieces of debris were seen coming from the vicinity of the payload bay and traveling up toward the Station. One of these pieces appeared to follow a curvilinear path past the Kristall array. Also, IMAX footage revealed a button-like object bouncing within the payload bay several minutes after docking.

None of the visible debris was seen making contact with the Mir structure. However, their trajectories could not be traced beyond the Station due to the debris exiting the camera field-of-view before possible contact could be verified.

One small piece of light-colored debris could be seen near the Base Block SP#2 array twenty minutes before docking on Figure 8-B. The particle traveled up in front of the array before exiting the camera's field-of-view. Its maximum width was estimated to be less than an inch in size. The particle did not appear to make contact with the Station.

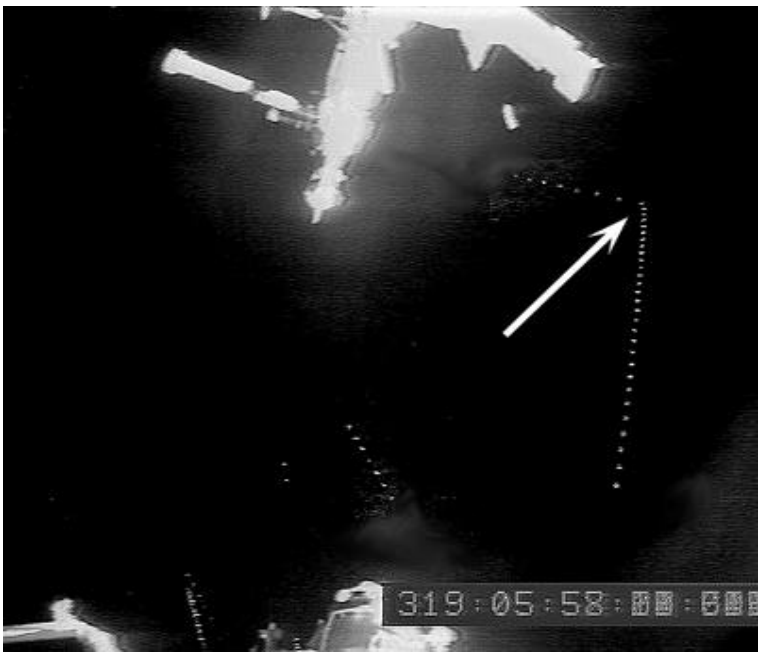

Figure 8-B Trajectory of Deflected Debris

Figure 8-B shows the trajectories of several pieces of debris during a 37 second period (at 1 second intervals) as seen from camera C. (Although C was a color camera, the time lapse display procedure required single-band imagery and results in a black and white image.) The particle identified with the arrow was one of two that appeared to be deflected by an apparent interaction with an Orbiter thruster plume. The initial velocity of this particular piece was estimated at approximately 15 inches per second. Both the speed and direction of the particle appeared to change, however, quantitative discussion of these measures would be very speculative. The sequence of Orbiter RCS thruster pulses that could have contributed to the particle's change in motion (at 319:05:58:12 GMT) is shown in Table 8-A.

Time	Orbiter RCS Jet Firings
319:05:58:11.838	R5R
319:05:58:11.918	R5R, L5D
319:05:58:12.078	L5D
319:05:58:12.558	F4D, L3D, R3D
319:05:58:12.638	F3D, L2D, R2D

Table 8-A Orbiter RCS Thruster Firings During Debris Deflection

8.1 Debris seen just prior to Docking

During the fifteen minutes just prior to docking, seven pieces were seen traveling toward the Mir Station. Several pieces were seen moving from the payload bay toward the Station before leaving the camera C field-of-view. The image below was acquired twenty minutes before docking with the Station, approximately seventy feet from the Orbiter.

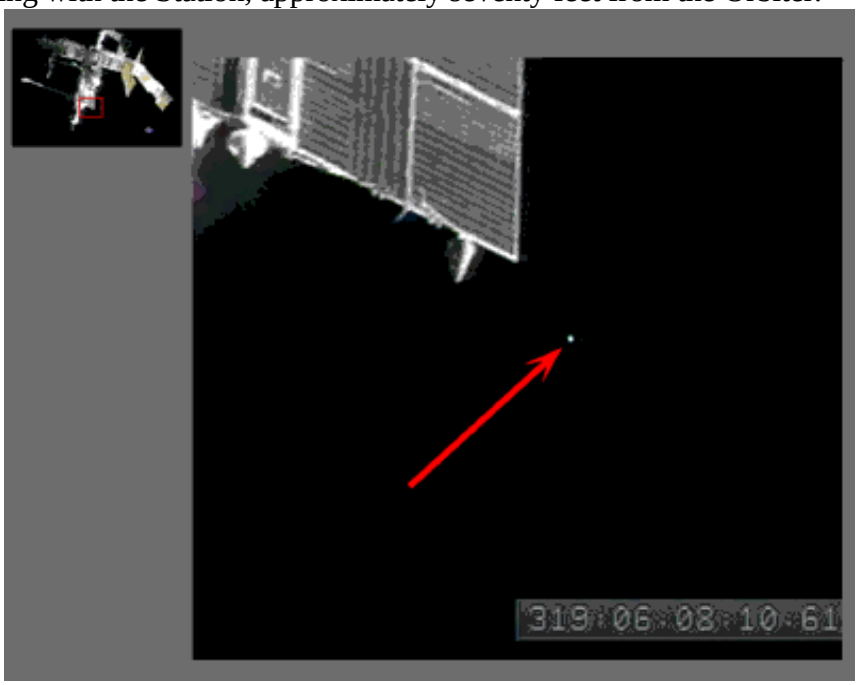

Figure 8-C Debris seen near Base Block SP#2 Array During Approach

Figure 8-C shows one small piece of light-colored debris near a Base Block SP#2 array twenty minutes before docking. The particle traveled up in front of the array before exiting the camera's field-of-view. Its maximum width was estimated to be less than an inch in size.

8.2 Debris near Docking Interface

In the interval between soft docking and hard mate, nine small pieces of light-colored debris were seen between Orbiter and Shuttle docking interfaces on elbow camera views. All of the visible debris were estimated to be smaller than 0.5 inches. One very small piece of light colored debris of unknown origin appeared to bounce off the surface below the Orbiter capture ring during the transition between the ready-to-dock and lock-up positions. Its velocity was estimated to be about 1 inch per second. No damage was apparent on the available views.

8.3 Debris seen just after Docking

After hard dock, nine more pieces of small light colored debris were seen traveling up toward the Mir Station from the general direction of the payload bay. The curved trajectory of the largest of these pieces is shown in Figure 8-D.

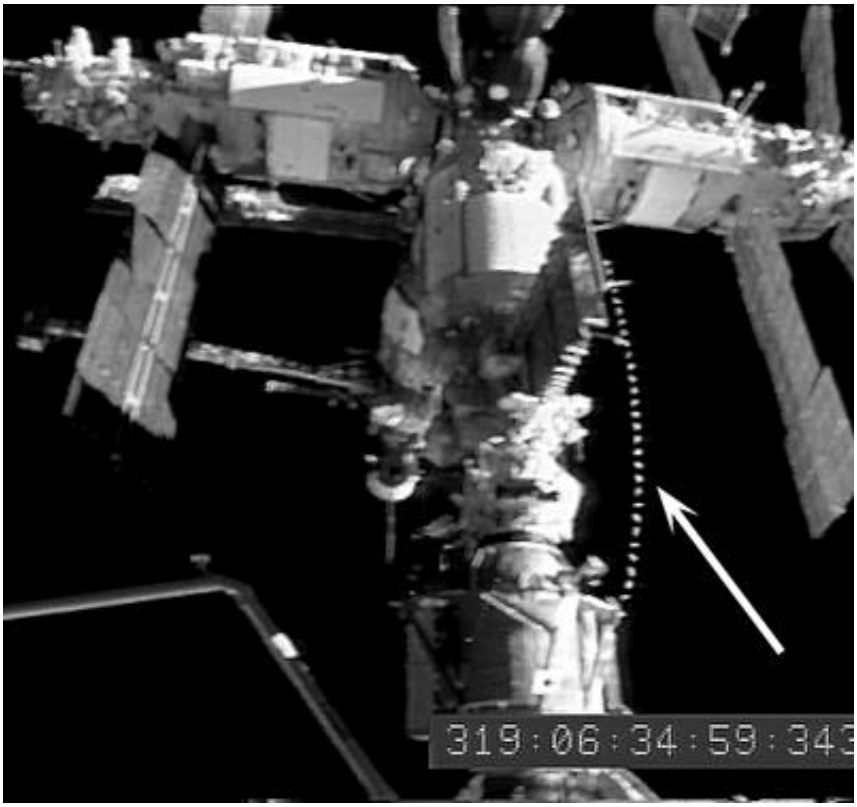

Figure 8-D Tumbling Debris seen after Docking

The debris shown in Figure 8-D appeared to tumble as it moved up across the camera's field-of-view. This composite image was also generated using a time lapse capture sequence over a 30 second interval using camera C. The particle's size was estimated to be approximately 2 inches along its largest dimension and its velocity to be about 9 inches/second. In addition, IMAX footage captured during the sequence revealed several small pieces of debris within the payload bay. One such piece of debris is shown in Figure 8-E.

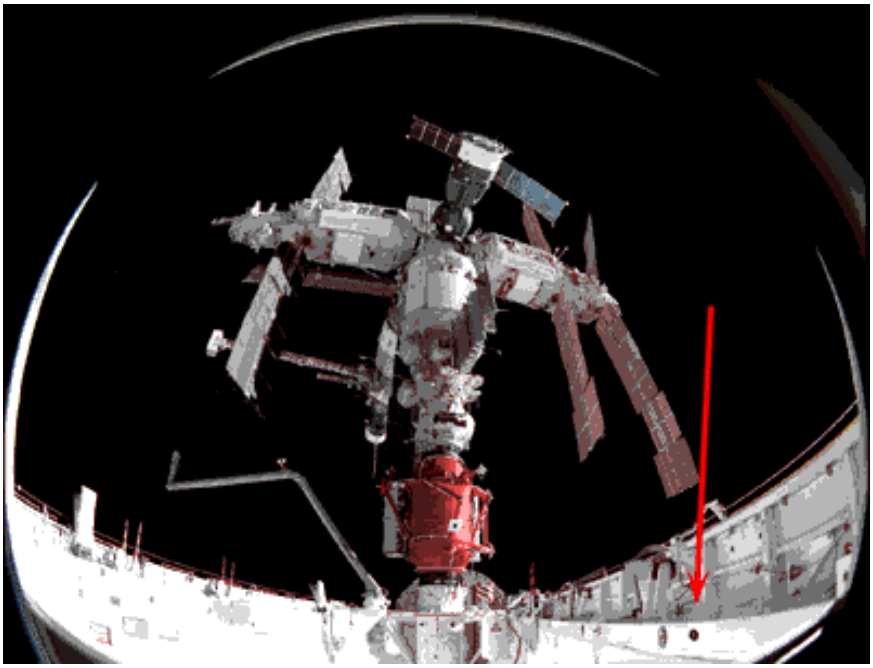

Figure 8-E IMAX view of Button Debris shortly after Docking

IMAX footage revealed this piece of debris (identified as a button used to fasten thermal blanket material) bouncing within the confines of the payload bay several minutes after docking. Figure 8-E shows this debris after it appeared to travel from the forward section of the payload bay to the rear. After hard dock, nine other pieces of small light colored debris were seen traveling up toward the Station. None were seen to make contact with Station surfaces while within the camera field-of-view.

8.4 Debris Assessment Error Analysis

Analysis of debris floating in space was limited by several factors including lighting conditions, field-of-view conflicts and camera control.

Lighting obviously plays a major role in the visibility of debris. During certain segments of the approach, sunlight was illuminating the Station at an oblique angle. Under these conditions, debris and propellant material from Orbiter thrusters were more clearly visible. Also, as the sun began to rise within an orbital pass, payload bay cameras (with lens apertures wide open) showed a saturated Mir Station but revealed particles that would not otherwise be seen. Unfortunately, the resultant "blooming" also made it difficult to obtain accurate measurements of the debris. The need for wide-angle views that show debris trajectories and plume interactions conflict with the need for zoomed-in views to characterize individual particles.

Available payload bay camera views were not always able to track each piece of debris to conclusively determine whether contact was made with Station surfaces. Since debris assessment usually involves analysis of unexpected events, the use of cameras to identify sources and follow trajectories was usually secondary to other events.

9. IMAGERY EVALUATION

This section discusses overall quality of the film and video data obtained during DTO-1118. Scenelists with detailed information about specific rolls of film and videotapes are included in Appendices B and C.

Imagery acquired of Mir surfaces during STS-74 consisted roughly of the following:

- 10 hours of downlink video
- 12 hours of onboard video
- 470 frames of 35 mm film
- 560 frames of 70 mm film
- 90 Electronic Still Camera (ESC) images

9.1 Video Review

Payload bay cameras provided complete coverage of the Docking Module installation prior to the rendezvous. All four cameras, along with centerline views, were used in the procedure.

The RMS elbow camera provided the first views of the Mir approximately seven hours before docking. Intermittent views from all four payload bay cameras were downlinked during the final 500 feet of approach. The CTVC camera in the centerline position provided continuous, excellent imagery between far approach and docking. During the night phase of the orbit, only the blinking lights on the docking mechanism were visible. Unique views of the final feet of approach were acquired from the RMS elbow camera located just in front of the port side of the Docking Module.

Much of the downlinked survey video was obtained via INCO ground control during three crew sleep periods of the docked phase. All four payload bay cameras, as well as the elbow camera, were used in acquiring Mir survey imagery. This footage provided excellent coverage of the Orbiter-facing sides of the Spektr, Kvant-2, Base Block and Kvant modules. In addition, systematic coverage of both the Kristall and the newly installed Docking Module were obtained. Detailed coverage of the docking module was obtained at the request of Mir Environmental Effects Payload (MEEP) investigators. The elbow camera was also used to survey the Kvant array. Investigators involved in the possible retrieval of a panel section from the Kvant array requested this data. The retrieval of a panel would occur before the entire array is jettisoned at a future date. In general, video coverage of array surfaces was better than that on previous missions because of sun angles and access to elbow camera views. Camera D was used to acquire imagery of Kvant-2 SP#2 array motion during one of three Primary Reaction Control System (PRCS) tests. The camera field-of-view was sufficient, but not optimal, to perform motion and frequency analysis. Camcorder video was primarily limited to flight deck views of crew activities.

The centerline camera provided good views of the Docking Module interface area for much of the backaway. Views were also obtained from camera D during the first few minutes of backaway. This camera was targeted to view possible Base Block array motion during

backaway. Some sun glare was visible on this view and made it difficult to discern motion. Fly-around coverage appeared to be spotty. Payload bay cameras A and D as well as the keel camera, were used to acquire data during fly-around. One of these scenes was able to capture the flexing of the Kvant array. Part of the fly-around did occur in darkness, and little useful information could be obtained from these views.

In general, payload bay camera views provided good overview imagery of the Station configuration. Camera and crew constraints limited acquisition of video data during proximity operations. Coverage of the PRCS test was not optimal due to a field-of-view setting that appeared to be too wide. CTVC cameras provided excellent imagery during the docked phase survey of the Mir Station.

9.2 Still Photography Review

While many views of the Mir were acquired using the Hasselblad (70mm), Nikon (35mm), and ESC cameras during approach, few showed close-up views of the docking area. Access to the overhead window hampered data acquisition during this time period.

Systematic coverage of the Orbiter-facing sides of the Progress, Kvant, and Base Block modules was obtained using the Hasselblad camera with the 100mm lens. The Nikon camera with the 180mm lens was used to get systematic coverage of the Kvant-2 and Spektr modules. However, neither the 250mm lens on the Hasselblad nor the 300mm lens on the Nikon was used extensively during the docked phase. Both cameras were used to capture imagery of module sides not seen previously. Several excellent images were also acquired of solar arrays from inside the Mir Station. Other still photography acquired was especially useful for analysis of surface features. One particular 35mm image of the Base Block extracted surface texture information by taking advantage of oblique lighting conditions. Other imagery of variably lit regions (such as end cones and nozzle areas) showed the advantages of exposure bracketing to reveal detail in each area.

No still film imagery of the Station was acquired during backaway. Only a few ESC frames of the Docking Module were obtained.

The 70mm camera was used to capture fly-around views of the Station. These provided adequate coverage of surfaces not seen during the docked phase. No 35mm footage was acquired. ESC frames provided much of the coverage during fly-around.

In general, the quality of the photography acquired on STS-74 was excellent. Views that took advantage of oblique lighting conditions were especially useful for surface feature analysis. Imagery acquired through Mir windows proved to be helpful in analyzing the condition of different arrays. The STS-74 crew was concerned that there was not enough film set aside for DTO-1118. Therefore, the amount of imagery they captured after undocking was limited. This film issue is currently being worked for future missions.

10. CONCLUSIONS AND RECOMMENDATIONS

The combined imagery gathered on the STS-63, STS-71, and STS-74 missions provide a significant amount of information from which an assessment can be made on the effects of the space environment to the Mir orbiting platform. STS-74 rendezvous imagery provides baseline coverage of the ($-Z_B$) sides of Kvant, Kvant-2, Spektr, and the Base Block which have not been seen before.

Systematic coverage of the Orbiter-facing sides of Mir modules were obtained on this mission. The following conclusions can be drawn from analyzing procedures and equipment used to acquire the film and video data:

- Through STS-74, approximately 90% overview (i.e., including video and long-range fly-around still photography) coverage of the Station has been obtained. This type of imagery was adequate to assess surface quality and for noting configuration discrepancies.
- Through STS-74, approximately 50% detailed (i.e., close-up still photography) coverage of the Station has been obtained. These pictures are used to measure the extent of possible orbital debris damage and discoloration to surface features on each module.
- The solar array motion events analyzed on STS-71 and STS-74 appear to be very different and uncorrelated.
- Systematic coverage of Station surface features with the 250mm lens has been limited on each mission.
- STS-74 crew members felt that the amount of film allotted for the survey should have been greater.
- Imagery acquired of the Docking Module during backaway was limited to ESC views due to this perceived lack of film.
- Use of INCO controlled payload bay cameras to perform surveys during sleep periods reduced the impact on crew time required.
- As on STS-71, ESC imagery was adequate for quick-look analysis, but did not provide enough detail for in-depth analysis.

10.1 Discussion of Results

The imagery gathered during the STS-74 Mir survey complemented that taken from both STS-63 and STS-71. The close-up view of the Spektr radiator facing the Orbiter provided excellent coverage of the blistering and chipping of paint on the surface of the radiator. Coverage of the Kvant SP #2 array (which had been on the ($+X_B$) side of Kristall prior to STS-71) provided close-up views of the damage sites seen on STS-71 imagery. Instead of surface delamination of a single cell, entire strips of cells can be seen lifted away from their underlying mesh support structure. Texture information on the surface of the Base Block is highlighted by light striking the surface at an oblique angle. These include features on the micrometeoroid sensor and other areas where discoloration has chipped off revealing a brighter surface below. The bracketing of exposure settings reveals detail in the relatively bright surfaces of the modules while also extracting features in the shadowed regions of module interfaces. The most significant example of bracketing provided detail on the

purge port at the base of Kvant and revealed a splay pattern at the base of Kvant and the end of the Base Block.

Survey video data was once again mainly used for the study of motion. No visible plume impingement was seen to any of the Mir arrays during approach. However, views of different arrays during the docked phase revealed motion not seen on earlier missions. The source of this motion did not appear to be plume impingement. Since this motion was unexpected, further study during future missions is warranted and will be emphasized. Video analysis was performed on one of the three PRCS tests. Results will be compared to those obtained by the PASDE experiment (whose results have not yet been released). Information from these tests can be used to verify structural dynamics models of the Shuttle/Mir docked configuration.

10.2 Recommendations

Each subsequent rendezvous mission will approach the Station from the same side as the STS-74 mission. This will provide a unique opportunity to view surfaces across a span of months and study the effects of the space environment on common features. STS-76 is presently scheduled to launch on March 21, 1996. Current plans call for a station-keep at 170 feet. This should allow acquisition of image data while the Mir orients the Docking Module toward the Orbiter. However, judging from past missions, the actual timing of this maneuver is not always predictable.

Based on crew comments during STS-76 training and evaluation of STS-74 imagery, the following recommendations have been made:

- Change the primary camera during proximity operations from the Hasselblad to the Nikon. This decision was based on crew comments that bracketing with the 35mm (Nikon) camera would be easier during non-static events and also because it would allow use of the 300mm lens during the fly-around.
- Map out the total number of views required with each specified lens to obtain complete coverage of the Station from available windows during the docked phase. This change was implemented to comply with film stowage and utilization requirements.
- Stress the use of the 250mm lens during crew training sessions to obtain more detailed surface coverage of Mir.
- Consider the use of a larger format camera or longer focal length lens on upcoming rendezvous missions for obtaining detailed coverage during fly-around.
- Continue to use ground control of payload bay video cameras to perform Mir surveys during crew sleep periods. This has been the most effective way of obtaining survey video footage and allows real-time decisions on target coverage.
- Continue to track debris around the Mir Station during rendezvous operations.
- Emphasize the need for bracketing exposures when acquiring imagery. STS-74 provided several examples where surface detail remained hidden until brought out with different aperture settings.
- Request the crew to be aware of lighting conditions that highlight surface features. Lighting angles oblique to Mir surfaces convey textural information that would otherwise remain hidden.

- Fill at least one video camera field-of-view with the Mir during fly-around. Unanticipated array motion, such as that seen with the Kvant on STS-74, will be easier to detect with this configuration.

11. REFERENCES

- Bluth, B. J., D. Fielder, Soviet Space Stations as Analogs, Vol. II, 3rd Edition, September 1993.
- Gaskill, J. D., *Linear Systems, Fourier Transforms, and Optics*, John Wiley & Sons, New York, New York, 1978.
- Lillesand, T. M., R. W. Kiefer, *Remote Sensing and Image Interpretation*, John Wiley & Sons, New York, New York, 1979.
- NASA/RSC-E Joint Report, Mir Photo/TV Survey (DTO-1118): STS-63, JSC-27246, August 28, 1995.
- NASA/RSC-E Joint Report, Mir Photo/TV Survey (DTO-1118): STS-71, JSC-27355 January 16, 1996.
- Mission Operations Directorate, Space Flight Training Division, Systems Training Branch, A Russian Space Station: The Mir Complex, National Aeronautics and Space Administration, Lyndon B. Johnson Space Center, Houston, Texas, February 1994.
- NASA Drawing Package, STS-74 Shuttle Mir Docking Mission, WG-3/RSC-E/NASA/003/3402-2, August 11, 1995.
- Portree, David S. F., Information Services Division, Mir Hardware Heritage, JSC 26770, Lyndon B. Johnson Space Center, Houston, Texas, October 1994.